

SEP 4 1973

ORNL
MASTER COPY

ORNL-TM-4207
R

FABRICATION AND CHARACTERIZATION OF
PLUTONIUM TEST ELEMENT FTE-13:
AN HTGR TEST ELEMENT CONTAINING
 PuO_{2-x} , $\text{Th}_{0.75}\text{Pu}_{0.25}\text{O}_{2-x}$, AND ThO_2

C. F. Sanders
J. D. Sease



OAK RIDGE NATIONAL LABORATORY
OPERATED BY UNION CARBIDE CORPORATION • FOR THE U.S. ATOMIC ENERGY COMMISSION

This report was prepared as an account of work sponsored by the United States Government. Neither the United States nor the United States Atomic Energy Commission, nor any of their employees, nor any of their contractors, subcontractors, or their employees, makes any warranty, express or implied, or assumes any legal liability or responsibility for the accuracy, completeness or usefulness of any information, apparatus, product or process disclosed, or represents that its use would not infringe privately owned rights.

Contract No. W-7405-eng-26

METALS AND CERAMICS DIVISION

FABRICATION AND CHARACTERIZATION OF PLUTONIUM TEST ELEMENT

FTE-13: AN HTGR TEST ELEMENT CONTAINING PuO_{2-x} ,

$\text{Th}_{0.75}\text{Pu}_{0.25}\text{O}_{2-x}$, AND ThO_2

C. F. Sanders J. D. Sease

AUGUST 1973

OAK RIDGE NATIONAL LABORATORY
Oak Ridge, Tennessee 37830
operated by
UNION CARBIDE CORPORATION
for the
U.S. ATOMIC ENERGY COMMISSION



CONTENTS

Abstract	1
Introduction	1
Fuel Design	1
Kernel Preparation	3
Coating	6
Fuel Rod Fabrication	13
Element Loading	17
Archives	17
Summary and Conclusions	17
Acknowledgments	18
Appendix A. Data Summary Coated Particle Sheets for Plutonium Test Element Project	19
Appendix B. Photographs of Coated Particles	27
Appendix C. Green and Annealed Rod Data	41
Appendix D. Photographs of Microstructure of Rods	51
Appendix E. Photographs of Fuel Rods for PTE	57



**FABRICATION AND CHARACTERIZATION OF PLUTONIUM TEST ELEMENT
FTE-13: AN HTGR TEST ELEMENT CONTAINING PuO_{2-x} ,
 $\text{Th}_{0.75}\text{Pu}_{0.25}\text{O}_{2-x}$, AND ThO_2 ¹**

C. F. Sanders² J. D. Sease

ABSTRACT

Plutonium is potentially a very attractive fuel for high-temperature gas-cooled reactors, in which it would replace makeup ^{235}U that is required when operating on the ^{233}U -Th fuel cycle. We developed a process and materials for the plutonium test element that is being irradiated in the Peach Bottom Reactor and fabricated the plutonium-bearing fuel components for it. The fuel element contained fissile kernels of PuO_2 and ThO_2 -25% PuO_2 prepared by sol-gel procedures. We applied successive layers of low-density isotropic carbon, high-density isotropic carbon, silicon carbide, and high-density isotropic carbon. Fabrication of fuel rods by the slug injection process produced a coated-particle body bound together by a carbonaceous binder. The report describes the fabrication and the characterization of these plutonium-bearing components.

INTRODUCTION

This is the final report on the fabrication of the plutonium-bearing fuel components for HTGR test element FTE-13, which is being irradiated in the Peach Bottom Reactor. These components were fabricated under a contract [AT-(40-1)-4226] with funds provided by the Edison Electric Institute (EEI) and Gulf General Atomic (GGA) Division of Gulf Energy and Environmental Systems, Inc. Gulf General Atomic designed and specified all the components for FTE-13. The design of FTE-13 is quite similar to that of 30 fuel test elements that are or have been installed in the Peach Bottom HTGR. Gulf General Atomic fabricated and assembled all the components for this element except for the plutonium fuel kernels and rods. The Oak Ridge National Laboratory developed processes and materials for the plutonium oxide fuel for this test element and then fabricated the plutonium-bearing fuel components for the element. This is the first plutonium fuel fabricated in this country for irradiation testing in an HTGR. This report describes the fuel design and the fabrication and inspection techniques used in kernel preparation, coating, fuel rod fabrication, and element assembly. The results of the inspections are discussed. The fabrication was accomplished between July 1971 and January 1972 without great difficulty, and the element was shipped to GGA during February 1972. The FTE-13 was inserted in Peach Bottom during the spring shutdown in May 1972. It is scheduled to be irradiated in Peach Bottom until the end of core II, which is now scheduled to operate until July 1974. The maximum burnups will be 43% FIMA in plutonium oxide particles and 10% FIMA in mixed-oxide particles. The fuel temperature will range from 2850 to 2170°F at the start of irradiation to 2440 to 1880°F at the end of core life. The maximum fast fluence will be 2.4×10^{21} neutrons/cm² (>0.1 MeV).

FUEL DESIGN

The plutonium-bearing fuel is in the form of coated microspheres of fissile particles containing plutonium and fertile particles of thorium oxide, bonded together by a carbonaceous matrix into a fuel rod approximately $\frac{1}{2}$ in. in diameter \times 2 in. long.

-
1. Work done for the USAEC under contract [AT-(40-1)-4226] with Gulf General Atomic Division of Gulf Energy and Environmental Systems, P.O. Box 608, San Diego, Calif. 92112.
 2. Now with Nuclear Fuels Division, Westinghouse Electric Corp., P.O. Box 5906, Columbia, S.C. 29205.

Table 1. Fuel loading of PTE fuel rods

Particle type	Kernel composition	Nominal kernel diameter (μm)	Oxygen-to-plutonium ratio, $2-x$	Thorium-to-plutonium ratio ^a	Plutonium loading (g Pu/in.)
Fissile kernel					
1	PuO_{2-x}	100	1.81	34	0.0839
2	$3\text{ThO}_2 \cdot \text{PuO}_{2-x}$	350	1.69	34	0.0804
4	PuO_{2-x}	200	1.68	31	0.0940
5	$3\text{ThO}_2 \cdot \text{PuO}_{2-x}$	350	1.84	36	0.0804
6	PuO_{2-x}	200	1.84	32	0.0940
Fertile kernel					
3	ThO_2	400			

^aIn mixture of fertile and fissile particles used in the fuel rods.

The coated-particle and fuel rod designs were specified by GGA. Particle design variables under study are kernel diameter, kernel composition, and coating design. The only specified fuel rod design variable was fissile particle type.

The plutonium-bearing fissile kernels are nominally 100- and 200- μm -diam PuO_{2-x} and 350- μm -diam $\text{ThO}_2-25\% \text{PuO}_{2-x}$. Different kernel sizes were chosen to provide data to verify models for predicting isotopic reaction rates of plutonium fuels in an actual HTGR environment. Information pertaining to particle coating design and thermal stability will be sought from the plutonium fuel particles having different oxygen-to-plutonium ratios and thorium dilution. Oxygen-to-plutonium ratios in the range 1.65 to 1.70 and 1.79 to 1.81 were specified for both the large-diameter PuO_{2-x} and the $(\text{Th,Pu})\text{O}_{2-x}$ kernels. The small PuO_{2-x} kernels were designed to the high oxygen-to-plutonium ratio of 1.79 to 1.81.

A TRISO³ coating was used for the fissile plutonium particles. This coating is similar to that on particles for the Fort St. Vrain Reactor.⁴ The various coating layer thicknesses were designed with the Kaae analytical stress model,⁵ and data from Flowers and Horsley⁶ on CO and fission gas generation in plutonium particles were input into the model for calculating the gas pressures in the particles. All particles were designed to survive under the most severe conditions expected in this irradiation test.

The fertile particles are of the type expected to be used in the large 1100-MW(e) HTGR. They are thorium oxide kernels with a BISO coating of pyrolytic carbon.

The various types of fissile particles are combined with fertile particles to make five fuel rod types. The fuel loading for FTE-13 is shown in Table 1.

The element contains 100 g of ^{235}U and 19 g of plutonium and will produce approximately 133 kW maximum. The maximum fuel particle burnups achieved will be in the center fuel body. Burnups of

3. TRISO and BISO are acronyms that denote the type of coating. TRISO contains three types of coating layers: low-density pyrolytic carbon around the kernel to act as a buffer and SiC and high-density isotropic pyrolytic carbon to retain the fission products. BISO contains two types of coating layers: low-density pyrolytic carbon buffer and high-density isotropic pyrolytic carbon to retain the fission products.

4. Oak Ridge National Laboratory and Gulf General Atomic, *National HTGR Fuel Recycle Development Program Plan*, ORNL-4702 (August 1971).

5. J. L. Kaae, "A Mathematical Model for Calculating Stresses in a Four-Layer Carbon-Silicon Carbide-Coated Fuel Particle," *J. Nucl. Mater.* 32, 322 (1969).

6. R. H. Flowers and G. W. Horsley, *The Influence of Oxide Kernels on the Manufacture and Performance of Coated Particle Fuel*, AERE-R-5949 (1968).

approximately 43% FIMA in the PuO₂ fissile particles and approximately 10% FIMA in the (Th,Pu)O₂ fissile particles will be achieved. It is planned to irradiate FTE-13 until the end of life for core II, or approximately 500 equivalent full-power days (EFPD), in core position E10-01.

The maximum fast fluence at the end of 500 EFPD will be approximately 2.4×10^{21} neutrons/cm² (>0.1 MeV), or about one-third of the expected fast fluence in a large HTGR. The design fuel temperatures will range from 2850 to 2170°F in the center fuel body at the start of irradiation, and from 2440 to 1880°F at the end of core life.

KERNEL PREPARATION

The plutonium-containing fuel kernels were prepared by ORNL sol-gel processes.^{7,8} The ThO₂-PuO₂ microspheres were made by mixing sols of the two constituents. After formation, the fissile microspheres were first sintered in argon to 1200°C, then heat treated at 1450°C in Ar-8% H₂ to adjust the oxygen-to-plutonium ratio.

Initial chemical analysis of the plutonium-containing microspheres showed the iron content to be greater than 500 ppm; therefore, all the microspheres were subsequently heat treated in vacuum at 1750°C. This heat treatment reduced the iron content to less than 500 ppm. The low oxygen-to-plutonium ratios were obtained by an additional heat treatment of those microspheres in pure hydrogen at 1750°C. The ThO₂ particles were prepared by the conventional ThO₂ sol-gel process in a cold laboratory.⁹

The characterization showed that the kernels were dense, round microspheres, and they met all the specifications of the contract. The properties are summarized in Table 2. The amounts of trace impurities as

7. R. G. Wymer, *Laboratory and Engineering Studies of Sol-Gel Processes at Oak Ridge National Laboratory*, ORNL-TM-2205 (May 1968).

8. J. P. McBride, *Laboratory Studies of Sol-Gel Process at Oak Ridge National Laboratory*, ORNL-TM-1980 (September 1967).

9. P. A. Haas, C. C. Haws, Jr., F. G. Kitts, and A. D. Ryon, *Engineering Development of Sol-Gel Processes at Oak Ridge National Laboratory*, ORNL-TM-1978 (January 1968).

Table 2. Summary of properties of kernels for plutonium test element

Particle type	Kernel composition	Diameter (μm)			Density		Iron ^c content (ppm)	O/Pu	EBC ^d (ppm)
		Range ^a	Average	σ	g/cm ³	% of theoretical ^b			
1	PuO _{2-x}	63-125	110	14	10.70	97.2	85	1.81	<2
2	(Th _{0.75} Pu _{0.25})O _{2-x}	295-420	349	31	9.90	97.2	291	1.69	<2
4	PuO _{2-x}	150-250	202	19	10.36	96.9	<50	1.68	<2
5	(Th _{0.75} Pu _{0.25})O _{2-x}	295-420	357	28	10.09	98.4	291	1.84	<2
6	PuO _{2-x}	150-250	181	23	10.80	95.7	85	1.84	<2

^aScreen cut.

^bTheoretical density calculated for plutonium oxide by $\rho = 10.952 + 0.506y - 2.4Z$, where y = atom fraction of Pu in heavy metal and $Z = 2.00 - \text{O/M ratio}$. For (Th,Pu)O₂ density of ThO₂ assumed to be 10.00 g/cm³; influence of Pu content calculated with previous formula.

^cIron content determined by quantitative wet chemical analysis; the approximate precision of the analysis is ±50 ppm.

^dEquivalent boron content determined using 2200 m/sec cross sections (ref: *Radiological Health Handbook* (rev. 1970), published by U.S. Department of Health, Education, and Welfare).

determined by emission spectrographic analysis are given in Tables 3 and 4. The results of plutonium isotopic analysis are given in Table 5. A sample of the (Th,Pu)O₂ microspheres was inspected for homogeneity and compositional variation from sphere to sphere and variation within the individual microspheres. To determine the variation from sphere to sphere, electron microprobe readings were taken from 25 different microspheres, and the results are shown in Fig. 1. To determine the variation in individual

Table 3. Mass spectrographic trace element analysis of (Th,Pu)O₂ (types 2 and 5)

Element	Content (ppm)	Element	Content (ppm)
Al	10	Nb	<1
As	<1	Ni	70
B	~0.7	P	30
Ba	1	Pb	<5
Bi	<1	Si	100
Ca	15	Sn	<3
Cd	<1	Sr	1
Co	≤1	Ti	~15
Cr	50	V	<1
Cs	N.D.	W	<10
Cu	0.3	Zn	<3
Fe ^a		Zr	<5
Hg	<5	Nd	15
Kr	3	Pr	2
Mg	20	Ce	20
Mn	~1	La	10
Mo	10	Y	30
Na	~3	S	50

^aSee Table 2.

Table 4. Trace element analysis of PuO₂ (types 1, 4, and 6)

Element	Content (ppm)		Element	Content (ppm)	
	63-125 μm	150-250 μm		63-125 μm	150-250 μm
Al	15	5	Na	20	20
B	0.5	0.5	Ni	150	500
Ba	10	10	P	200	500
Ca	20	50	Si	~300	~300
Co	1	1	Sr	<5	<5
Cr	~1000	~300	Th	10	70
Cu	20	20	Ti	100	100
Fe ^a			V	1	1
K	<5	<5	Zn	10	<10
Mg	15	15	Zr	3	3
Mn	30	30	S	50	50
Mo	20	20	Cl	50	100

^aSee Table 2.

microspheres, traverses along the radius of several microspheres were made, taking data at 10- μ m intervals. A typical set of data is shown in Fig. 2. Analysis of the microprobe results indicated that the microspheres were homogeneous, within the sensitivity of microprobe analysis. Photomicrographs of the kernels are shown in Fig. 3. The plutonium microspheres were etched using a solution of $Ce(NO_3)_3$ and HF, and the mixed-oxide kernels were etched with a boiling solution of H_3PO_4 and HF. The etched plutonium kernels

Table 5. Chemical and isotopic analysis of plutonium used in the plutonium test element

Material	% Pu	Particle type	Plutonium shipment	Content of each isotope (%)					
				238	239	240	241	242	244
$Pu(NO_3)_4$ soln		2, 5	12	<0.03	88.58	9.96	1.36	0.101	<0.0005
PuO_2 - ThO_2 sol	22.3	2, 5	12	<i>a</i>	<i>a</i>	<i>a</i>	<i>a</i>	<i>a</i>	<i>a</i>
PuO_2 - ThO_2 sol	22.3	2, 5	15	<i>a</i>	<i>a</i>	<i>a</i>	<i>a</i>	<i>a</i>	<i>a</i>
$Pu(NO_3)_4$ soln		2, 5	15	<0.045	88.87	9.73	1.25	0.14	<0.0001
PuO_2 sol (63-125)	88.2	1	15	0.047	88.73	9.84	1.241	0.144	0.001
$Pu(NO_3)_4$ soln		4, 6	14	0.03	88.69	10.01	1.20	0.104	<0.001
PuO_2 sol (150-250)	88.2	4, 6	14	0.033	88.77	9.95	1.144	0.107	0.0007

^aNot determined on microspheres.

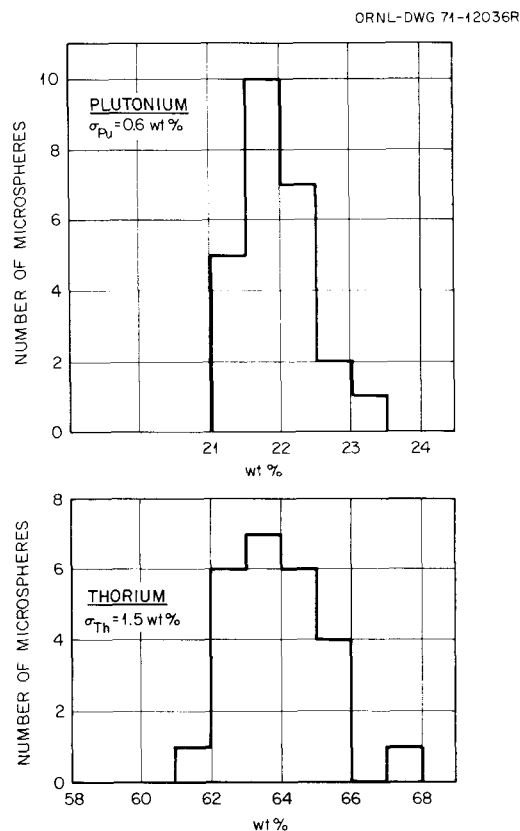


Fig. 1. Compositional variation of $(Th,Pu)O_2$ microspheres.

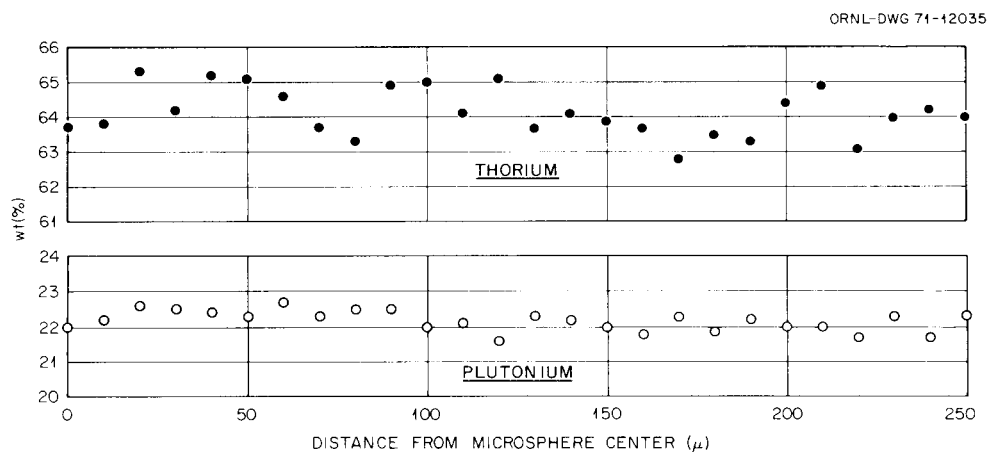


Fig. 2. Compositional variation within (Th,Pu) O_2 microsphere.

as seen in Fig. 3 show the two-phase nature of PuO_{2-x} . From the plutonium-oxygen phase diagram,¹⁰ these two phases are probably α - Pu_2O_3 and $PuO_{1.98}$, and the concentrations of the two phases with varying oxygen-to-metal ratios are about as one would predict from the phase diagram.

The photomicrographs of the plutonium kernels show a different arrangement of the two phases between the center of the kernels and the outer surfaces, which could be caused by the differential cooling between the inner and outer areas. The photomicrographs of the mixed-oxide kernels show them to be dense, with small grains and no detectable second phase. The defect areas, which can be seen on outside edges of some of the microspheres, are attributed to metallographic preparation.

The thoria microspheres were fabricated according to the standard ORNL flowsheet. The kernels are dense, round microspheres, and they met all of the specifications except that the equivalent boron content (EBC) was approximately 50 ppm.

COATING

The plutonium-containing kernels were coated in glove-box equipment especially designed for handling plutonium. Equipment for pyrolytic carbon coating of the plutonium existed at ORNL. Procedures and equipment for SiC coating of plutonium fuels were developed for FTE-13. The major equipment problem in coating the plutonium fuel for FTE-13 was associated with the disposal of the effluent from the silicon carbide coating process. When silicon carbide coatings are being deposited, the effluent consists of H_2 , HCl, and residual methyltrichlorosilane ($SiCH_3Cl_3$). Early attempts to dispose of the effluents by reacting with wetted aluminum chips failed. A dry scrubber composed of granular Ascarite¹¹ and Drierite¹² in cartridge form proved to be very effective. Ascarite, which is asbestos saturated with NaOH, and Drierite, which is $CaSO_4$, were mixed in approximately four parts Ascarite to one part Drierite and were loosely packed in a Pyrex tube to form the scrubber.

10. T. D. Chikalla, C. E. McNeilly, and R. E. Skandakal, "The Plutonium-Oxygen System," *J. Nucl. Mater.* **12**(2), 131-41 (1964).

11. Supplied by A. H. Thomas Company.

12. Supplied by W. A. Hammond.

ETCHED

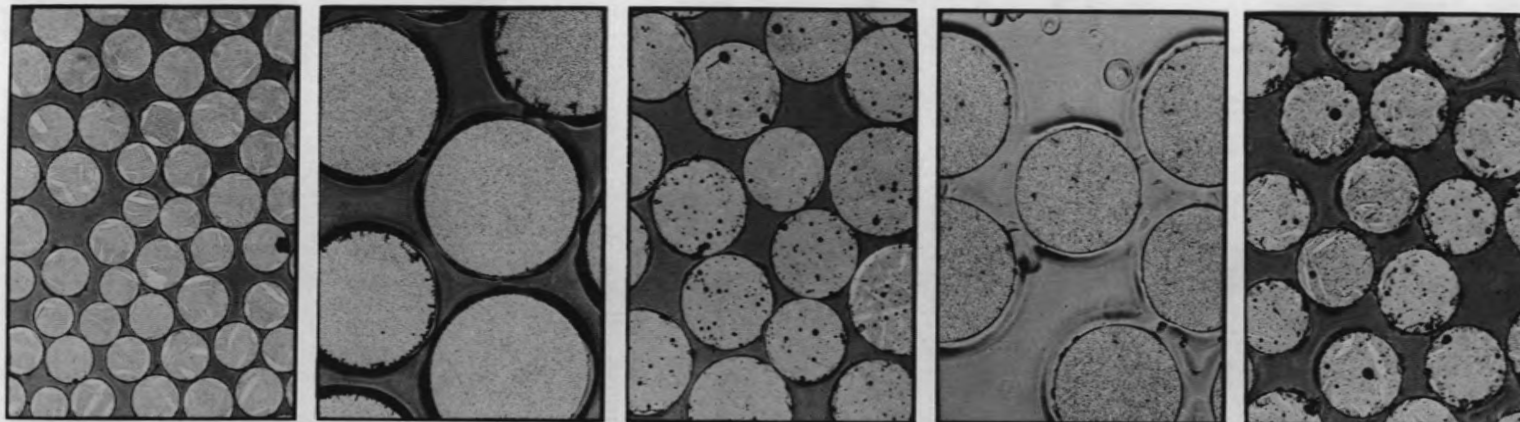
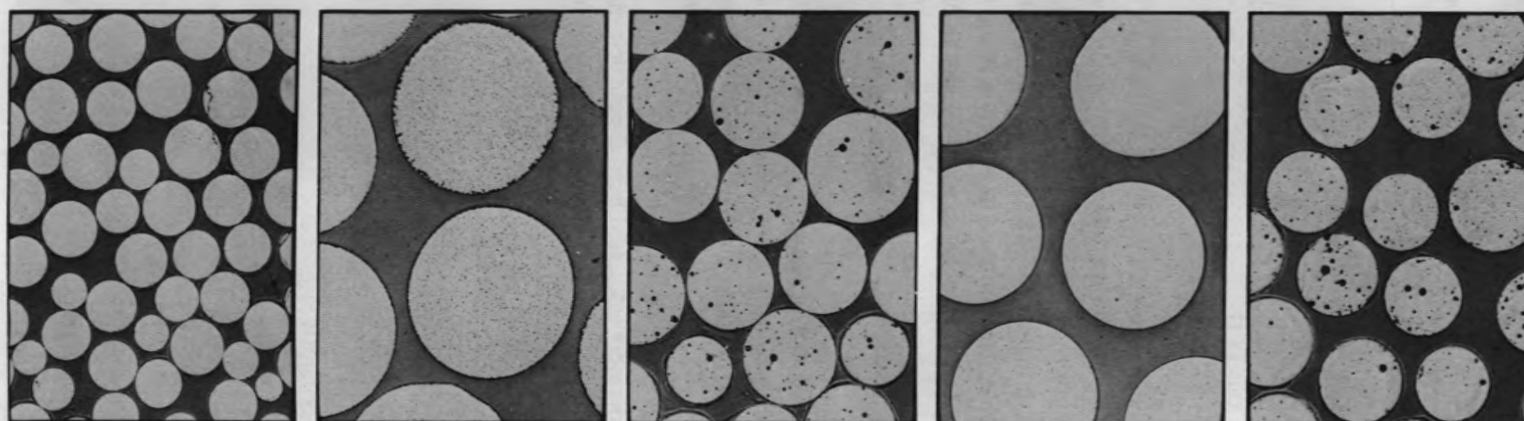
AS
POLISHEDITEM
KERNEL
Th/Pu1
 $\text{PuO}_{1.81}$
0/12
 $\text{ThO}_2/\text{PuO}_{1.69}$
3/14
 $\text{PuO}_{1.678}$
0/15
 $\text{ThO}_2/\text{PuO}_{1.84}$
3/16
 $\text{PuO}_{1.84}$
0/1

Fig. 3. Fissile kernels for plutonium test element. 65X.

Table 6. General coating conditions for FTE-13 plutonium fuel kernels

Coating	Coating temperature (°C)	Reacting gas	Reacting gas flux (cm ³ min ⁻¹ cm ⁻²)	Diluent gas (vol %)
Buffer	1000–1050	C ₂ H ₂	3–5	20–27
Buffer sealer	1300–1375	C ₃ H ₆	0.6–0.7	83
Inner LTI	1300–1375	C ₃ H ₆	2.5–3.0	0–36
SiC	1500–1550	CH ₃ SiCl ₃	0.01–0.03	98
Outer LTI	1300–1400	C ₃ H ₆	1.5–2.1	40–42

The FTE-13 fuel materials were coated in a 1³/₄-in.-diam single-inlet coating chamber. The carbon coatings were the conventional low-temperature isotropic coatings¹³ (LTI) derived from propylene with the low-density buffer derived from acetylene. The SiC coatings were obtained from methyltrichlorosilane with hydrogen as the carrier gas. The general coating conditions are shown in Table 6.

The only problem encountered in coating was the difficulty with the 100- μ m PuO₂ particles (type 1). To coat the small PuO₂ particles, it was necessary to dilute the bed with larger (250- to 300- μ m) ThO₂ for the first two coating operations. We solved the cleanliness problem by taking care never to expose the freshly coated particles to any plutonium-contaminated surface and by keeping the last particle-handling box clean.

The coating densities, coating thicknesses, microstructure, plutonium concentration, and fraction of defective particles were of primary importance in characterizing the coated particles. Plutonium kernel coatings along with the design specifications are summarized in Table 7. The coating specifications were met in essentially all cases. Where coating specifications were not met, GGA judged that these deviations would have no significant effect on performance.

Buffer densities were calculated from the particle dimensions and densities of the inner LTI coating, the kernel, and the particle according to the following equation:

$$\rho_B = \frac{\rho_{TOT}D_I^3 - \rho_K D_K^3 - \rho_I(D_I^3 - D_B^3)}{D_B^3 - D_K^3}, \quad (1)$$

where

ρ_B = buffer density,

ρ_I = inner LTI coating density,

ρ_{TOT} = particle density after buffer and inner LTI coatings,

ρ_K = kernel density,

D_I = particle diameter after inner LTI coating,

D_K = kernel diameter,

D_B = particle diameter after buffer coating.

13. R. L. Beatty, J. L. Scott, and D. Kiplinger, *Minimizing Thermal Effects in Fluidized-Bed Deposition of Dense, Isotropic Pyrolytic Carbon*, ORNL-4531 (April 1970).

Table 7. Properties of FTE-13 coatings

Particle type	Buffer	Inner LTI	SiC	Outer LTI	Total coating
Coating thickness, μm					
1 Design	50–60	15–20	20–30	25–35	120–140
Mean	49	19	21	25	114
2 Design	80–95	25–35	30–40	50–60	195–220
Mean	94	43	37	46	220
3 Design	55–75			65–85	130–150
Mean	64			78	142
4 Design	80–95	20–30	35–45	30–40	175–200
Mean	79	32	39	35	185
5 Design	80–95	25–35	30–40	50–60	195–220
Mean	91	36	30	53	210
6 Design	80–95	20–30	35–45	30–40	175–200
Mean	93	24	41	38	196
Coating density, g/cm^3					
Design	1.0–1.3	1.7–1.9	≥ 3.18	1.7–1.9	
1 Mean	0.76	1.900	3.219	1.410	
2 Mean	0.981	1.743	3.216	1.865	
3 Mean	1.08			1.921	
4 Mean	0.99	1.833	3.202	1.845	
5 Mean	1.24	1.789	3.220	1.816	
6 Mean	1.39	1.798	3.201	1.821	

The above calculation involves the third power of the various diameters, thus multiplying the experimental error involved in the diameter measurements. Therefore, the calculated buffer density should be considered approximate. Of the five particle types, only types 3 and 5 had buffer densities that met specifications; the others did not. The densities for the LTI pyrolytic carbons and the SiC layers were determined with a density gradient column technique.¹⁴ Because of the penetration of the liquid suspension media into the LTI pyrolytic carbons, the densities of the outer LTI's were checked by a mercury pycnometer burn technique. Table 8 compares the two techniques for three samples.

It can be seen that the pycnometer results yield a significantly lower density than does the gradient column technique. A more detailed statistical analysis of the coating densities is given in Appendix A.

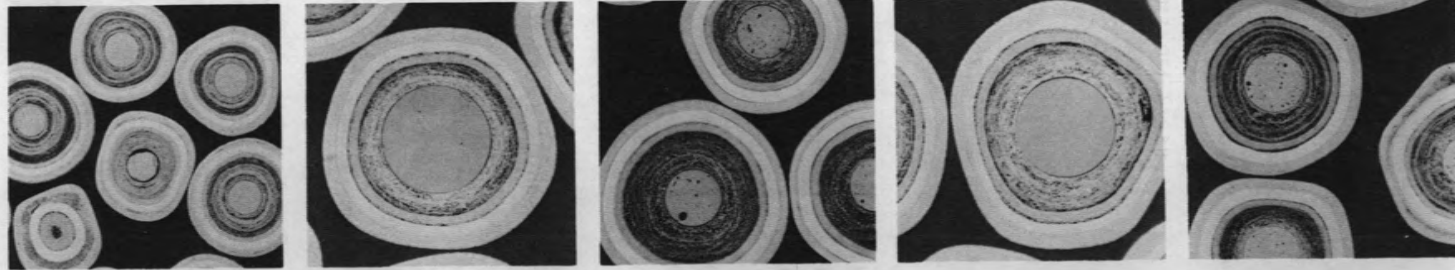
The coating thickness for the various layers was determined by microradiography. The sealer layers could not be measured on metallographic samples because these layers were not anisotropic. The mean coating thicknesses for the six particle types are summarized in Table 7, and a more detailed statistical analysis is given in Appendix A.

Metallographic photographs of the coated fissile particles in bright-field and polarized light are shown in Fig. 4. Close metallographic examination showed the coating to be essentially isotropic and within GGA's visual specifications, except for the 100- μm PuO₂ kernels. These particles had a higher than specified amount of oriented porosity in the outer LTI coating. However, this condition was judged not to be

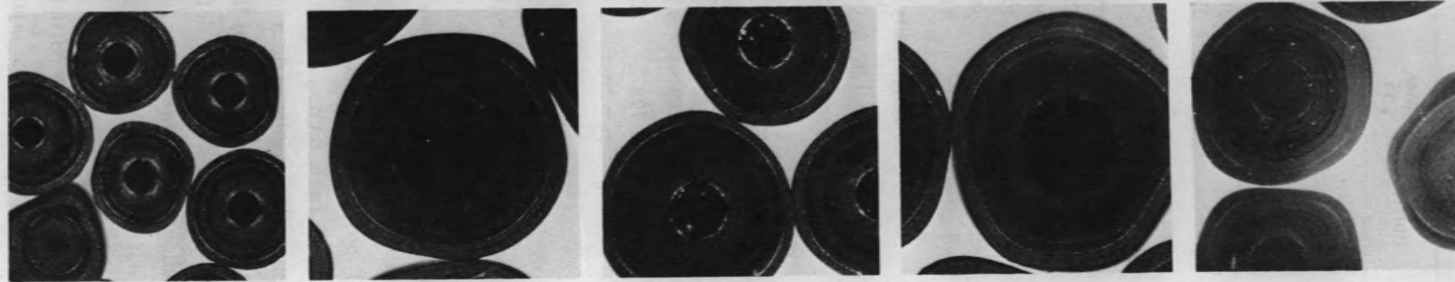
14. D. C. Canada and W. R. Laing, "Use of a Density Gradient Column to Measure the Density of Microspheres," *Anal. Chem.* 39, 691–92 (1967).

0.035 in.
100 x

BRIGHT
FIELD



POLARIZED
LIGHT



ITEM
KERNEL
Th/Pu

1
PuO_{1.81}
0/1

2
ThO₂/PuO_{1.69}
3/1

4
PuO_{1.68}
0/1

5
ThO₂/PuO_{1.84}
3/1

6
PuO_{1.84}
0/1

Fig. 4. Microstructure of coated fissile particles for FTE-13.

Table 8. Comparison of coating densities determined by a density gradient column with results obtained with a mercury pycnometer

Coating run	Density, by gradient column (g/cm ³)	Density, g/cm ³ , by mercury pycnometer		
		15 psi	10,000 psi ^a	15,000 psi
OR-1651	1.798	1.685		1.786
Pu-268	1.865	1.710	1.807	
Pu-269	1.816	1.71	1.799	

^aFor plutonium-bearing samples the available mercury pycnometer is limited to 10,000 psi.

Table 9. Impurity levels in particle coatings

Element	Semiquantitative content, ppm, for each particle type					
	1	2	3	4	5	6
Al	0.7	0.5	0.2	0.2	<0.1	0.5
B	<0.1	<0.1	<0.1	<0.1	<0.1	<0.1
Ca	2	2	0.8	8	8	8
Cb	130	0.3	0.1	10		0.2
Cr	130	0.3	0.1	10		1
Cu		2	2	5	0.5	20
Fe	5	1	0.3	1	1	1
K	0.3	2	0.2	0.2	0.1	20
Mg		0.5	≤1	5	0.5	1
Na		<0.5	<0.5	<0.5	<0.5	0.5
Ni	1	0.5	0.2	2	≤0.5	0.2
Si	Major	100	1	Major	600	1000
Sr	0.2					
P		0.2	0.2	<0.1	0.2	<0.1
S	2	4	<1	<1	<1	1

detrimental to the performance of the particles for this test and, therefore, they were accepted. A more complete set of photographs is given in Appendix B.

The impurity levels in the particle coatings given in Table 9 were determined by spark source mass spectroscopy.¹⁵ In this technique several particles are mounted in an electrode tip and sparked to give successive exposures of increasing duration until the kernels are reached. The coating process did not add appreciable contamination.

The surface contamination was determined by alpha counting the particles and applying a geometric correction factor of 2. The fractional surface contamination was then calculated by

$$\frac{\text{g Pu on surface}}{\text{g Pu total}} = \frac{\alpha_c}{(\text{wt \% Pu}/100) (N\lambda f)}, \quad (2)$$

15. "Standard Methods for Chemical, Mass Spectrometric, and Spectrochemical Analysis of Nuclear-Grade Mixed Oxides [(U,Pu)O₂]," ASTM-C698-72A, in *Annual Book of ASTM Standards*, Part 32, American Society for Testing and Materials, Philadelphia, 1972.

where

α_c = alpha count corrected for geometry,

N = Avogadro's number divided by molecular weight,

f = atom fraction of isotope,

λ = $\ln 2$ /half-life = decay constant.

The nuclear constants used for the plutonium-bearing materials were those for the three main isotopes, ^{239}Pu , ^{240}Pu , and ^{241}Pu . The resulting fractional surface contaminations are given in Table 10. All the surface contamination levels were well below the 2×10^{-6} and 1×10^{-4} allowed for plutonium and thorium respectively.

Considerable difficulties were encountered in determining plutonium in the coated fissile particles by chemical analysis within the required 5%. Most of the difficulties were associated with the presence of the SiC coatings, which greatly complicated the dissolution step. As an independent check, the plutonium content was calculated from radiographic measurements of kernel and particle diameters, the plutonium content of the kernels, and the particle densities before and after coating. The plutonium content from these two methods is compared in Table 11.

Table 10. Surface contamination levels for coated particles

Allowable levels are
Pu, 2×10^{-6} ; Th, 1×10^{-4}

Particle type	Surface contamination (g/g heavy metal)
1	3×10^{-8}
2	8×10^{-10}
3	$\sim 10^{-10}$
4	4×10^{-8}
5	2×10^{-11}
6	6×10^{-8}

Table 11. Comparison between chemical and geometric plutonium determinations

Particle type	Plutonium, wt %, by	
	Chemical analysis ^a	Geometric analysis ^a
1	9.97 ± 2.1	10.1 ± 0.81
2	6.96 ± 0.21	7.25 ± 0.32
4	18.26 ± 1.2	19.1 ± 0.93
5	7.8 ± 0.31	7.42 ± 0.31
6	16.54 ± 0.42	16.73 ± 0.87

^aThe \pm values indicate 95% confidence interval on the mean.

Defective SiC coatings were detected by burning off the outer coating and subjecting the burned particles to mercury at a pressure of 1000 psi. Any cracks 0.17 μm wide would be penetrated, and the cracked particles would be infiltrated by mercury. Then the particles were radiographed to determine if mercury infiltrated the SiC coatings. A radiographic examination of several thousand particles of each type revealed no defective SiC coatings.

From the examination of the microradiographs, we noted that approximately 1% of the coated particles from the 200- μm plutonium oxide kernels (types 4 and 6) showed some fuel migration after SiC coating. After 1800°C heat treatment to simulate the annealing step in rod fabrication, the frequency of detectable migration increased to 5 to 10% of these particles. Knowing the conditions of this irradiation test, we considered that this amount of fuel migration will not significantly affect the test.

FUEL ROD FABRICATION

The slug-injection¹⁶ process was selected for fuel rod fabrication instead of the hot-intrusion process because it appeared to be significantly simpler. The processes and equipment necessary to fabricate and inspect the FTE-13 fuel rods had to be developed, and special plutonium glove-box equipment for both fabrication and inspection had to be designed, fabricated, installed, and tested. The carbonization step required the development of a scrubber and off-gas system for glove-box operation. A schematic of the off-gas system for the carbonization step is shown in Fig. 5. The fission-gas release test required special designs and safety analysis to irradiate the plutonium fuel rods in the ORR and the setting up of a special glove box for annealing and fission-gas collection.

A reference Fort St. Vrain Reactor matrix obtained from GGA was used for all fuel rods. This matrix is a mixture of Asbury 6353 natural flake graphite and Allied Chemical Company 15V coal tar pitch. Analysis at ORNL showed the graphite filler content to be 28.7 wt %.

The type 2, 4, 5, and 6 fuel rods were molded by the slug-injection technique,¹⁶ which is shown schematically in Fig. 6. The particles were loaded into a cold mold, and a preformed slug of matrix was placed on top of them. After a top punch was inserted, the entire mold assembly was heated to 150°C; then a pressure of 750 psi was applied to force the molten matrix down through the interstices of the particle bed. Excess matrix was extruded through a radial orifice at the bottom of the mold. After cooling to about 20°C, the fuel rod was ejected from the mold.

The type 1 rods could not be fabricated by the slug-injection process, because the matrix could not be injected into the particle bed containing a blend of 350- and 680- μm coated particles. These rods were fabricated by the Admix process. Granular matrix (250 to 420 μm) was blended with the coated particles in a fluidized bed and loaded into the mold. The mixture was warm pressed at 150°C and 750 psi. The length, diameter, and weight of each fuel rod were determined after molding.

After forming, the fuel rods were supported vertically by Al_2O_3 powder in $\frac{5}{8}$ -in.-square holes in a webbed graphite boat and carbonized in argon to 800°C. They were then annealed in argon at 1800°C for 0.5 hr.

The axial distribution of graphite filler, the distribution of fissile and fertile particles, fuel rod dimensions, matrix density and microstructure, and fission gas release were of primary importance in characterizing the fuel rods.

16. R. A. Bradley, C. F. Sanders, and D. D. Cannon, *GCR and Thorium Utilization Programs Annu. Progr. Rep. Sept. 30, 1971*, ORNL-4760, pp. 52-55.

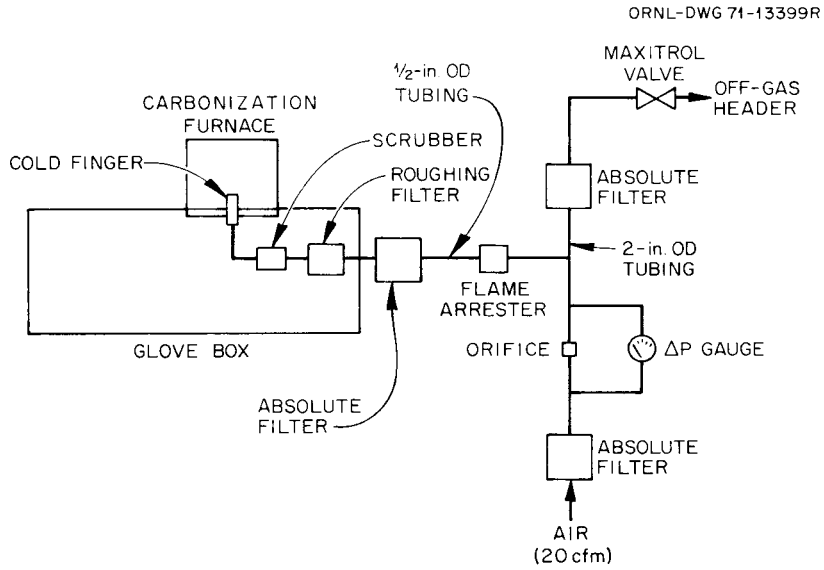


Fig. 5. Off-gas system for a carbonization furnace operating with a glove box.

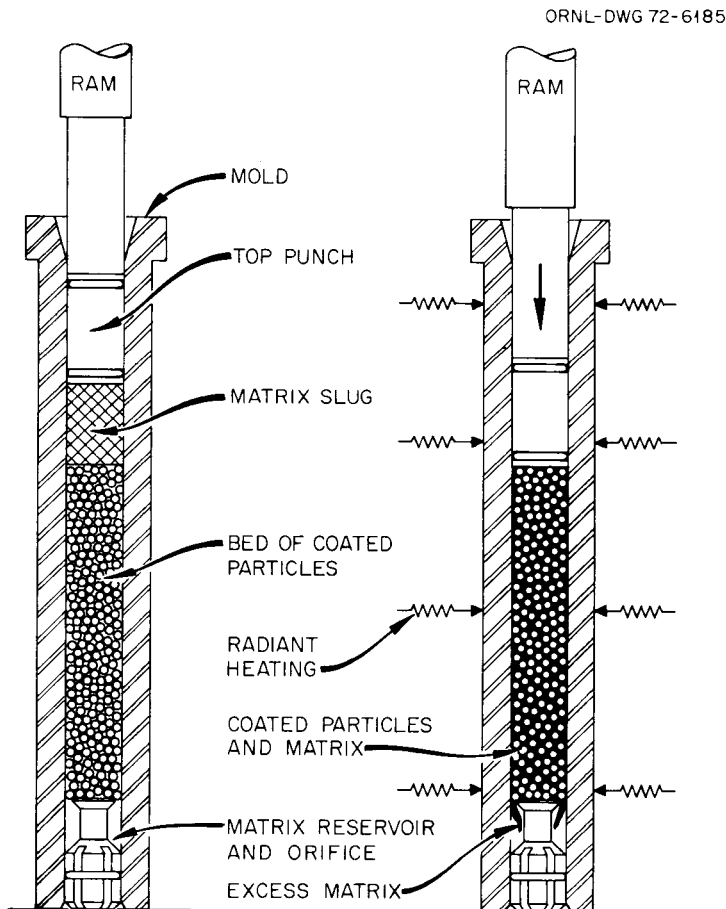


Fig. 6. Slug technique for making bonded-bed fuel rods.

Table 12. Results of graphite filler analyses on plutonium test element fuel rods

Fuel type	Filler content, wt %, for each location on two rods				
	Top	Middle	Bottom	Rod av ^a	Type av ^b
1	29.0, 29.8	27.9, 27.9	27.0, 27.1	28.0, 28.3	28.1
2	25.4, 26.0	31.1, 31.4	27.1, 27.6	27.9, 28.3	28.1
4	27.2, 26.8	27.7, 26.3	27.1, 26.8	27.3, 26.6	27.0
5	29.3, 30.2	29.6, 27.7	28.1, 27.5	29.0, 28.5	28.7
6	29.0, 28.3	27.3, 27.9	27.6, 27.0	28.0, 27.7	27.9
Position av	28.1 ± 0.9	28.5 ± 0.9	27.5 ± 0.9		

^a95% confidence interval on the rod average \bar{X}_r is $\bar{X}_r \pm 1.8$.

^b95% confidence interval on the type average \bar{X}_t is $\bar{X}_t \pm 1.2$.

The specifications for the fuel rods fabricated for the plutonium test element (GGA Specification FMB-2) state that the filler content in the injected matrix shall not vary from the nominal content of the mix more than 2 wt % over the fuel rod length. The axial distribution of graphite filler in slug-injected fuel rods was determined by breaking green fuel rods into three approximately equal sections, dissolving the matrix in pyridine, and separating the insoluble graphite. The results of these analyses, which are given in Table 12, indicate no significant variation in filler content along the rod.

After annealing, the maximum and minimum diameters at each end and the center of each rod were measured. The dimensional control of the fuel rods was extremely good. Within a given rod and between rods, variation was 0.001 in., and no rod was rejected because of diameter variations. The dimensions, matrix density, and particle packing fraction of the green and annealed fuel rods actually loaded in holes 1 through 8 of the PTE are given in Appendix C. The in situ coking value of the pitch, determined from weight loss of the rod during carbonization and annealing, is also included for each rod.

A metallographically prepared longitudinal section of one fuel rod from each particle type was examined to estimate the amount and distribution of macroporosity and the nature of the microporosity. The amount of macroporosity was less than the specified limit of 40 vol % for all types, and there were no concentrations of microporosity. No broken particles were apparent in the rods examined. Appendix D contains photographs for each particle type.

The distribution of the plutonium particles in the fuel rods was determined by gamma spectrometry. The samples were prepared by breaking the rods into sections, dissolving the matrix, and loading the particles into sample holders. The results of the distribution inspection are given in Table 13. The normalized plutonium content was calculated by the following formula:

$$Pu = \frac{\text{count rate of sample} / \text{wt of sample}}{\text{count rate of rod} / \text{wt of rod}}$$

From the above formula, a homogeneous rod would have a normalized plutonium content of 1. In most cases the homogeneity requirement was not met; these results point out the difficulties of blending various sizes of microspheres.

The fission gas release was determined by irradiating the rods to approximately 10^{14} fissions, heating the sample to 1100°C, collecting the gases, and determining the amount of ^{85m}Kr in the gas sample by

Table 13. Fissile particle distribution in fuel rods for FTE-13

Particle type	Position	Normalized Pu content		
		Sample "A"	Sample "B"	Average
Measured by gamma counting				
2	Top	1.07	0.96	1.015
2	Bottom	0.94	1.07	1.005
5	Top	1.12	1.14	1.13
5	Bottom	0.83	0.88	0.855
6	Top	1.28	1.24	1.26
6	Bottom	0.78	0.82	0.80
4	Top	1.10	1.15	1.125
4	Bottom	0.92	0.84	0.88
1	Top	1.13	1.13	1.13
1	Bottom	0.88	0.89	0.885
Measured by sizing and weighing				
1	Top	1.13	1.09	1.11
1	Bottom	0.84	0.91	0.875

Table 14. Fission gas release and surface contamination on fuel for the plutonium test element

Particle type	Fission gas released ^a (^{85m} Kr released/ ^{85m} Kr produced)	Surface ^b contamination (dpm/g)
1	9.8×10^{-6}	1.0×10^4
2	5.3×10^{-6}	5.5×10^2
4	1.2×10^{-4}	6.5×10^4
5	1.0×10^{-6}	5.8×10^2
6	3.7×10^{-5}	2.9×10^4

^aMeasurement taken on fuel rods.^bMeasurement taken on coated particles.

gamma spectrometry. The number of fissions was calculated from the yields of the fission products ¹³²Te, ¹³¹I, and ¹⁴⁰Ba. The mixed oxides (types 2 and 5) had a gas release of about 10⁻⁶, and the rods containing coated particles with undiluted plutonium had gas releases above 10⁻⁵. The results of the fission gas release on the rods and the alpha counting of the coated particles are listed in Table 14. Since the alpha activity of the plutonium oxide kernels is approximately two orders of magnitude higher than the alpha activity of the mixed-oxide kernels, we believe that most of the fission gas release is due to plutonium contamination of the coated particle.

Table 15. Loading for plutonium test element

Hole	Fissile particle type	Stack height (in.)	Distance from top of fuel rods to top of element (in.)
1	5	27.28	2.721
2	6	27.23	2.798
3	6	27.24	2.784
4	1	27.16	2.888
5	1	27.15	2.859
6	4	27.10	2.906
7	2	27.17	2.855
8	5	27.33	2.691
Total weight of loaded element			5045 g
Smears, α d/m			<30
Total weight of polystyrene			2.6 g
Distance from top of sample holder "A" to top of element			18 in.
Distance from top of sample holder "B" to top of element			12 $\frac{3}{16}$ in.

ELEMENT LOADING

The plutonium test fuel element was loaded with fuel without any difficulties. After loading, no alpha contamination was detected on the exterior surfaces of the fuel element. The loading data are summarized in Table 15. The plutonium fuel element was sent to GGA during February 1972. The plutonium fuel element, along with the top and bottom fuel elements fabricated at GGA, was incorporated into the Peach Bottom test element during March 1972. Appendix E contains photographs of each rod that was loaded.

ARCHIVES

Archive samples of the bare kernels, coated particles, and fuel rods are stored in bird cage 102-1570 in the Fuel Cycle Technology (FCT) Alpha Laboratory at ORNL. Supporting data and records on each fabrication step are filed in the FCT laboratory at ORNL.

SUMMARY AND CONCLUSIONS

The fuel for the first test of plutonium in an HTGR in this country has been fabricated at ORNL under a program jointly sponsored by Gulf General Atomic and the Edison Electric Institute. The fabrication was accomplished between July 1971 and January 1972, without great difficulty, and the fuel met essentially all the specifications.

This program revealed a number of areas for further process and quality control development; however, there are no foreseeable limitations to full-scale fabrication of plutonium fuels for use in HTGR's. The main areas for further development in quality control are plutonium analysis, oxygen-plutonium determination after coating, coating anisotropy, and broken particle fraction.

ACKNOWLEDGMENTS

The funds for the fabrication of the plutonium test element were provided jointly by Gulf General Atomic and the Edison Electric Institute. This project could not have been completed successfully without the dedicated and diligent efforts of many people. We would like to particularly acknowledge P. R. Kasten, D. A. Nehrig, A. L. Lotts, T. Gulden, and J. L. Scott for overall supervision and coordination. The kernels were prepared by W. T. McDuffie and F. G. Kitts under the direction of R. G. Wymer. The particles were coated by C. E. DeVore and H. Keating under the direction of C. B. Pollock and E. S. Bomar, with the assistance of D. M. Hewette and W. H. Pechin. The fuel rods were fabricated by W. H. Miller and W. B. Stines under the direction of R. A. Bradley. Also, we would like to acknowledge the personnel who were responsible for the characterization, in particular, J. H. Cooper, J. Bolt, and D. A. Costanzo of the Analytical Chemistry Division; H. R. Gaddis, E. H. Lee, and B. C. Leslie of the Metallography Group, Metals and Ceramics Division; C. W. Cunningham of the Reactor Division; M. T. Morgan of the Reactor Chemistry Division; and W. J. Mason of the Nondestructive Testing Group, Metals and Ceramics Division.

APPENDIX A

Data Summary Coated Particle Sheets for Plutonium Test Element Project

Appendix A contains detailed characterization of the coated particles for the Plutonium Test Element project. In particular, more detailed statistical data are listed. This includes a 95% confidence limit for the mean and limits for the permitted percentile as given in FMB-1, Issue B. The upper limits for the permitted percentile for the particular item are also given. If this limit is equal to or greater than the limit for the permitted percentile given in FMB-1, the item meets or exceeds the requirement. The limits not meeting requirements have been circled.

DATA SUMMARY COATED PARTICLES SHEETS FOR:

Item No. 1 For Experiment FUTE Batch No. Pu-286 Kernel Mat'l PuO_{1.81}

Layer Run No.	Parameter	Design Value	Mean	Standard Deviation	n	Confidence Limit	Critical Region	
							Permitted Percentile	Limit at Percentile
Kernel:	Diameter (μm)	<u>65-125</u>	<u>110</u>	<u>10</u>	<u>25</u>	<u>106-114</u>	<u>NA</u>	<u> </u>
<u>H-219</u>	Density (g/cm ³)	<u> </u>	<u>10.7</u>	<u> </u>	<u> </u>	<u> </u>	<u>NA</u>	<u> </u>
Buffer:	Thickness (μm)	<u>50-60</u>	<u>49</u>	<u>11</u>	<u>25</u>	<u>44-53</u>	<u>1.0</u>	<u>(14)</u>
<u>Pu-283</u>	Density (g/cm ³)	<u>1.0-1.3</u>	<u>(0.76)</u>	<u>ND</u>	<u> </u>	<u> </u>	<u>NA</u>	<u> </u>
Sealer:	Thickness (μm)	<u>1-3</u>	<u>ND</u>	<u> </u>	<u> </u>	<u> </u>	<u> </u>	<u> </u>
<u>Pu-283</u>	Thickness (μm)	<u>1-3</u>	<u>ND</u>	<u> </u>	<u> </u>	<u> </u>	<u> </u>	<u> </u>
Inner Carbon Coating:	Thickness (μm)	<u>15-20</u>	<u>19</u>	<u>5</u>	<u>25</u>	<u>17-22</u>	<u>1.0</u>	<u>(3)</u>
<u>Pu-285</u>	Density (g/cm ³)	<u>1.7-1.9</u>	<u>1.900</u>	<u>0.01</u>	<u>13</u>	<u>1.894-1.906</u>	<u>NA</u>	<u> </u>
<u>Pu-285</u>	OPTAF	<u> </u>	<u>NM</u>	<u> </u>	<u> </u>	<u> </u>	<u> </u>	<u> </u>
SiC:	Thickness (μm)	<u>20-30</u>	<u>21</u>	<u>2</u>	<u>25</u>	<u>21-22</u>	<u>1.0</u>	<u>15</u>
<u>SC-Pu-149</u>	Density (g/cm ³)	<u>≥3.18</u>	<u>3.219</u>	<u>0.001</u>	<u>9</u>	<u>3.218-3.220</u>	<u>1.0</u>	<u>3.215</u>
Outer Carbon Coating:	Thickness (μm)	<u>25-35</u>	<u>25</u>	<u>5</u>	<u>25</u>	<u>23-27</u>	<u>1.0</u>	<u>(9)</u>
<u>Pu-286</u>	Density (g/cm ³)	<u>1.7-1.9</u>	<u>1.910</u>	<u>0.020</u>	<u>10</u>	<u>1.896-1.924</u>	<u>ND</u>	<u> </u>
<u>Pu-286</u>	OPTAF	<u> </u>	<u> </u>	<u> </u>	<u> </u>	<u> </u>	<u> </u>	<u> </u>

Surface Contamination (g/g)	<u>6.023 × 10⁻⁹</u>	<u>Particle Composition</u>	<u>Isotope</u>	<u>Atom %</u>		
Density by	Particle	Coating	Wt % Pu	<u>9.62</u>	<u>Pu-238</u>	<u>0.047</u>
15 psi	<u>2.232</u>	<u>1.727</u>	Wt % Th	<u>NA</u>	<u>Pu-239</u>	<u>88.73</u>
75 psi	<u> </u>	<u> </u>	Wt % U	<u>NA</u>	<u>Pu-240</u>	<u>9.84</u>
10,000 psi	<u>2.275</u>	<u>1.811</u>	Wt % C	<u>54.08</u>	<u>Pu-241</u>	<u>1.241</u>
Defective SiC (fraction):	<u>None</u>		Wt % O	<u>ND</u>	<u>Pu-242</u>	<u>0.001</u>
Missing or incomplete layers (fraction)	<u>None</u>		Wt % Si	<u>ND</u>		
			Other	<u> </u>		
			Boron Equiv (ppm)	<u><0.1</u>	} for coating only	
			Iron (ppm)	<u>5</u>		
Coating microstructure and shape:	<u>Accept</u>	<u>See below</u>	<u>Reject</u>	<u> </u>		
Fission gas release R/B:	<u> </u>					
Metallographic Data:	Spec. No. <u>P-668</u>	Photo No. <u> </u>	Radiographic Plate No. <u>Pu-286</u>			
Comments:	<u>SiC deposited in two steps; coating thickness after first was not sufficient.</u>					
	<u>Batch Pu-286 had 15% unacceptable porosity in outer layer.</u>					

NA = not applicable ND = not determined. Properties not meeting requirements are circled.

DATA SUMMARY COATED PARTICLES SHEETS FOR:

(Th/Pu)_{0.6}Item No. 2For Experiment FUTEBatch No. Pu-268Kernel Mat'l 311

Layer Run No.	Parameter	Design Value	Mean	Standard Deviation	n	Confidence Limit	Critical Region	
							Permitted Percentile	Limit at Percentile
Kernel:	Diameter (μm)	295-420	346	31	25	332-358	NA	
H-218	Density (g/cm ³)		10.09	ND			NA	
Buffer:	Thickness (μm)	80-95	94	8	25	90-97	1.0	69
Pu-266	Density (g/cm ³)	1.0-1.3	0.98	ND			NA	
Sealer: Pu-266	Thickness (μm)	1-3	ND					
Inner Carbon	Thickness (μm)	25-35	29	5	50	38-49	1.0	13
Coating: Pu-266	Density (g/cm ³)	1.7-1.9	1.743	0.0105	15	1.737-1.749	NA	
	OPTAF		ND					
SiC: SC-139	Thickness (μm)	30-40	37	13	25	42-32	1.0	28
	Density (g/cm ³)	≥3.18	3.216	0.003	10	3.231-3.206	1.0	3.201
Outer Carbon	Thickness (μm)	50-60	46	10	25	50-42	1.0	14
Coating: Pu-268	Density (g/cm ³)	1.7-1.9	1.865	0.009	17	1.860-1.870		
	OPTAF	NM						

Surface Contamination (g/g)	4.69×10^{-12}		Particle Composition	Isotope	Atom %
Density by	Particle	Coating	Wt % Pu	Pu-238	<0.033
15 psi	2.588	1.71	Wt % Th	Pu-239	88.66
75 psi			Wt % U	Pu-240	9.9
10,000 psi	2.637	1.807	Wt % C	Pu-241	1.302
Defective SiC (fraction):			Wt % O	Pu-242	0.122
Missing or incomplete layers (fraction)			Wt % Si	Pu-244	<0.001
			Other		
			Boron Equiv (ppm)	<0.1 } for coating	
			Iron (ppm)	1 } only	
Coating microstructure and shape:	Accept	X	Reject		
Fission gas release R/B:	NM				
Metallographic Data:	Spec. No. P-659	Photo No.	Radiographic Plate No. Pu-268		
Comments:					

NA = not applicable ND = not determined. Properties not meeting requirements are circled.

DATA SUMMARY COATED PARTICLES SHEETS FOR:

Item No. 3 For Experiment PUTE Batch No. OR-1686 Kernel Mat'l ThO₂

Layer Run No.	Parameter	Design Value	Mean	Standard Deviation	n	Confidence Limit	Critical Region	
							Permitted Percentile	Limit at Percentile
Kernel:	Diameter (μm)	<u>350-400</u>	<u>413</u>	<u>14</u>	<u>25</u>	<u>407-418</u>	<u>NA</u>	<u> </u>
<u>B-C-3</u>	Density (g/cm ³)	<u> </u>	<u>10</u>	<u> </u>	<u> </u>	<u> </u>	<u>NA</u>	<u> </u>
Buffer:	Thickness (μm)	<u>55-75</u>	<u>64</u>	<u>7</u>	<u>25</u>	<u>67-61</u>	<u>1</u>	<u>42</u>
<u>OR-1686</u>	Density (g/cm ³)	<u>1.0-1.3</u>	<u>1.08</u>	<u>ND</u>	<u> </u>	<u> </u>	<u>NA</u>	<u> </u>
Sealer:	Thickness (μm)	<u>1-3</u>	<u>ND</u>	<u> </u>	<u> </u>	<u> </u>	<u> </u>	<u> </u>
Inner Carbon	Thickness (μm)	<u>NA</u>	<u> </u>	<u> </u>	<u> </u>	<u> </u>	<u> </u>	<u> </u>
Coating:	Density (g/cm ³)	<u>NA</u>	<u> </u>	<u> </u>	<u> </u>	<u> </u>	<u> </u>	<u> </u>
	OPTAF	<u>NA</u>	<u> </u>	<u> </u>	<u> </u>	<u> </u>	<u> </u>	<u> </u>
SiC:	Thickness (μm)	<u>NA</u>	<u> </u>	<u> </u>	<u> </u>	<u> </u>	<u> </u>	<u> </u>
	Density (g/cm ³)	<u>NA</u>	<u> </u>	<u> </u>	<u> </u>	<u> </u>	<u> </u>	<u> </u>
Outer Carbon	Thickness (μm)	<u>65-85</u>	<u>78</u>	<u>6</u>	<u>25</u>	<u>81-76</u>	<u>1</u>	<u>59</u>
Coating:	Density (g/cm ³)	<u>1.7-1.9</u>	<u>1.921</u>	<u>0.003</u>	<u>13</u>	<u> </u>	<u> </u>	<u> </u>
<u>OR-1686</u>	OPTAF	<u>ND</u>	<u> </u>	<u> </u>	<u> </u>	<u> </u>	<u> </u>	<u> </u>

Surface Contamination (g/g) <u>~10⁻¹⁰</u>			Particle Composition		Isotope	Atom %
Density by	Particle	Coating	Wt % Pu	<u>NA</u>	<u>ND</u>	<u> </u>
15 psi	<u>3.37</u>	<u>ND</u>	Wt % Th	<u>53.9</u>	<u> </u>	<u> </u>
75 psi	<u>3.38</u>	<u>ND</u>	Wt % U	<u>NA</u>	<u> </u>	<u> </u>
10,000 psi	<u>3.49</u>	<u>ND</u>	Wt % C	<u>46.4</u>	<u> </u>	<u> </u>
Defective SiC (fraction):	<u>NA</u>		Wt % O	<u>ND</u>	<u> </u>	<u> </u>
Missing or incomplete layers (fraction)	<u>None</u>		Wt % Si	<u>NA</u>	<u> </u>	<u> </u>
			Other	<u> </u>	<u> </u>	<u> </u>
			Boron Equiv (ppm)	<u> </u>	<u><0.1 for coating</u>	<u> </u>
			Iron (ppm)	<u> </u>	<u>0.3 only</u>	<u> </u>
Coating microstructure and shape:	Accept	<u>X</u>	Reject	<u> </u>	<u> </u>	<u> </u>
Fission gas release R/B:	<u>ND</u>					
Metallographic Data:	Spec. No. <u>72546</u>	Photo No. <u> </u>	Radiographic Plate No. <u>OR-1686</u>			
Comments:	<u>The particles of this batch were consumed before all fuel rods were made.</u>					
	<u>Therefore, another batch of material, OR-1692, was made.</u>					

NA = not applicable ND = not determined. Properties not meeting requirements are circled.

DATA SUMMARY COATED PARTICLES SHEETS FOR:

Item No. 3 For Experiment PUTE Batch No. OR-1692 Kernel Mat'l ThO₂

Layer Run No.	Parameter	Design Value	Mean	Standard Deviation	n	Confidence Limit	Critical Region	
							Permitted Percentile	Limit at Percentile
Kernel:	Diameter (μm)	<u>350-400</u>	<u>396</u>	<u>17</u>	<u>25</u>		<u>NA</u>	
<u>B-C-3</u>	Density (g/cm ³)		<u>10</u>				<u>NA</u>	
Buffer:	Thickness (μm)	<u>55-75</u>	<u>64</u>	<u>9</u>	<u>25</u>			
<u>OR-1692</u>	Density (g/cm ³)							
Sealer:	Thickness (μm)	<u>1-3</u>	<u>ND</u>					
<u>OR-1692</u>								
Inner Carbon	Thickness (μm)							
Coating:	Density (g/cm ³)							
<u>NA</u>	<u>OPTAF</u>							
SiC:	Thickness (μm)							
<u>NA</u>	Density (g/cm ³)							
Outer Carbon	Thickness (μm)	<u>65-85</u>	<u>70</u>	<u>5</u>	<u>25</u>	<u>72-68</u>	<u>1</u>	
Coating:	Density (g/cm ³)							
<u>OR-1692</u>	<u>OPTAF</u>	<u>1.7-1.9</u>	<u>1.91</u>	<u>0.010</u>	<u>20</u>	<u>1.915-1.905</u>		

Surface Contamination (g/g)	<u>~10¹⁰</u>	Particle Composition	Isotope	Atom %
Density by	Particle	Coating	Wt % Pu	<u>NA</u>
15 psi	<u>3.36</u>	<u>ND</u>	Wt % Th	<u>55</u>
75 psi	<u>3.37</u>	<u>ND</u>	Wt % U	<u>NA</u>
10,000 psi	<u>3.47</u>	<u>ND</u>	Wt % C	<u>45</u>
Defective SiC (fraction):	<u>NA</u>	Wt % O	<u>ND</u>	
Missing or incomplete layers (fraction)	<u>None</u>	Wt % Si	<u>ND</u>	
		Other		
		Boron Equiv (ppm)	<u>1</u>	for coating
		Iron (ppm)	<u>30</u>	only
Coating microstructure and shape:	Accept <u>X</u>	Reject		
Fission gas release R/B:				
Metallographic Data:	Spec. No. <u>72568</u>	Photo No.		Radiographic Plate No. <u>OR-1692</u>
Comments:				

NA = not applicable ND = not determined. Properties not meeting requirements are circled.

DATA SUMMARY COATED PARTICLES SHEETS FOR:

Item No.	4		For Experiment	PUTE	Batch No.	Pu-282	Kernel Mat'l	PuO _{1.68}		
Layer Run No.	Parameter	Design Value	Mean	Standard Deviation	n	Confidence Limit	Critical Region			
							Permitted Percentile	Limit at Percentile		
Kernel:	Diameter (μm)	150-250	190	17	25	197-183	NA			
H-221	Density (g/cm ³)		10.36	ND			NA			
Buffer:	Thickness (μm)	80-95	79	17	25	72-86	1.0	25		
Pu-275	Density (g/cm ³)	1.0-1.3	0.99	ND						
Sealer:	Thickness (μm)	1-3	ND							
Pu-275	Inner Carbon Coating: Density (g/cm ³)	20-30	32	4	25	33-30	1.0	19		
	OPTAF	1.7-1.9	1.833	0.010	10	1.840-1.826	NA			
Pu-275	SiC: Thickness (μm)	35-45	39	2	25	38-40	1.0	33		
Sc-Pu-145	Density (g/cm ³)	>3.18	3.202	0.001	10	3.203-3.201	1.0	3.196		
Outer Carbon Coating:	Thickness (μm)	30-40	35	4	25	37-34	1.0	22		
	Density (g/cm ³)	1.7-1.9	1.845	0.015	21	1.852-1.838				
Pu-282	OPTAF	ND								
Surface Contamination (g/g)			9×10^{-11}			Particle Composition		Isotope	Atom %	
Density by	Particle	Coating				Wt % Pu	18.24	Pu-238	0.033	
15 psi		2.012				Wt % Th	NA	Pu-239	88.77	
75 psi						Wt % U	NA	Pu-240	9.95	
10,000 psi		2.125				Wt % C	46.11	Pu-241	1.144	
Defective SiC (fraction):			None			Wt % O	ND	Pu-242	0.107	
Missing or incomplete layers (fraction):			None			Wt % Si	ND	Pu-244	0.0007	
						Other				
						Boron Equiv (ppm)	<0.1	for coating		
						Iron (ppm)	1	only		
Coating microstructure and shape: Accept						X	Reject			
Fission gas release R/B: ND										
Metallographic Data: Spec. No. P-665						Photo No.	Radiographic Plate No. Pu-282			
Comments:										

NA = not applicable ND = not determined. Properties not meeting requirements are circled.

DATA SUMMARY COATED PARTICLES SHEETS FOR:

Item No.	5		For Experiment	PUTE		Batch No.	Pu-269		Kernel Mat'l	1(Th/Pu)O ₂ 3/1	
Layer Run No.	Parameter	Design Value	Mean	Standard Deviation	n	Confidence Limit	Critical Region		Permitted Percentile	Limit at Percentile	
Kernel:	Diameter (μm)	295-420	343	23	25	351-333	NA				
H-220	Density (g/cm ³)		9.9	ND							
Buffer:	Thickness (μm)	80-95	91	9	25	94-87	1.0		63		
	Density (g/cm ³)	1.0-1.3	1.24								
Sealer:	Thickness (μm)		ND								
Inner Carbon Coating:	Thickness (μm)	25-35	36	4	25	37-34	1.0		23		
	Density (g/cm ³)	1.7-1.9	1.789	0.011	15	1.796-1.781	NA				
	OPTAF	ND									
SiC:	Thickness (μm)	30-40	30	1	25	31-29	1.0		27		
	Density (g/cm ³)	>3.18	3.220	0.0033	11	3.222-3.218	1.0		3.206		
Outer Carbon Coating:	Thickness (μm)	50-60	53	4	25	55-52	1.0		40		
	Density (g/cm ³)	1.7-1.9	1.816	0.0179	18	1.825-1.807					
	OPTAF	ND									
Surface Contamination (g/g)			4×10^{-12}			Particle Composition		Isotope	Atom %		
Density by	Particle	Coating	Wt % Pu		7.82	Pu-238		<0.033			
15 psi	2.618	1.710	Wt % Th		ND	Pu-239		88.66			
75 psi			Wt % U		NA	Pu-240		9.90			
10,000 psi	2.671	1.799	Wt % C		46.07	Pu-241		1.302			
Defective SiC (fraction):			None		Wt % O	ND	Pu-242		0.122		
Missing or incomplete layers (fraction)			None		Wt % Si	ND	Pu-244		<0.001		
					Other						
					Boron Equiv (ppm)	<0.1		for coating			
					Iron (ppm)	1		only			
Coating microstructure and shape:			Accept	X	Reject						
Fission gas release R/B:			ND								
Metallographic Data:			Spec. No.	P-660	Photo No.	Radiographic Plate No.		Pu-269			
Comments:											

NA = not applicable ND = not determined. Properties not meeting requirements are circled.

DATA SUMMARY COATED PARTICLES SHEETS FOR:

Item No. 6 For Experiment PUTE Batch No. Pu-274 Kernel Mat'l PuO_{1.84}

Layer Run No.	Parameter	Design Value	Mean	Standard Deviation	n	Confidence Limit	Critical Region	
							Permitted Percentile	Limit at Percentile
Kernel:	Diameter (μm)	<u>150-250</u>	<u>198</u>	<u>14</u>	<u>25</u>	<u>204-193</u>	<u>NA</u>	<u> </u>
<u>H-217</u>	Density (g/cm ³)	<u> </u>	<u>10.8</u>	<u>ND</u>	<u> </u>	<u> </u>	<u> </u>	<u> </u>
Buffer:	Thickness (μm)	<u>80-95</u>	<u>93</u>	<u>15</u>	<u>25</u>	<u>99-87</u>	<u>1.0</u>	<u>45</u>
<u>Pu-271</u>	Density (g/cm ³)	<u>1.0-1.3</u>	<u>1.39</u>	<u>ND</u>	<u> </u>	<u> </u>	<u>ND</u>	<u> </u>
Sealer:	Thickness (μm)	<u>1-3</u>	<u>ND</u>	<u> </u>	<u> </u>	<u> </u>	<u> </u>	<u> </u>
<u>Pu-271</u>	Thickness (μm)	<u>1-3</u>	<u>ND</u>	<u> </u>	<u> </u>	<u> </u>	<u> </u>	<u> </u>
Inner Carbon	Thickness (μm)	<u>20-30</u>	<u>24</u>	<u>2</u>	<u>25</u>	<u>25-23</u>	<u>1.0</u>	<u>18</u>
Coating:	Density (g/cm ³)	<u>1.7-1.9</u>	<u>1.798</u>	<u>0.017</u>	<u>17</u>	<u>1.807-1.789</u>	<u>NA</u>	<u> </u>
<u>Pu-271</u>	OPTAF	<u>ND</u>	<u> </u>	<u> </u>	<u> </u>	<u> </u>	<u> </u>	<u> </u>
SiC:	Thickness (μm)	<u>35-45</u>	<u>41</u>	<u>2</u>	<u>25</u>	<u>41-40</u>	<u>1.0</u>	<u>35</u>
<u>Pu-SC-143</u>	Density (g/cm ³)	<u>≤3.18</u>	<u>3.201</u>	<u>0.001</u>	<u>7</u>	<u>3.202-3.200</u>	<u>1.0</u>	<u>3.195</u>
Outer Carbon	Thickness (μm)	<u>30-40</u>	<u>38</u>	<u>4</u>	<u>25</u>	<u>40-37</u>	<u>1.0</u>	<u>25</u>
Coating:	Density (g/cm ³)	<u>1.7-1.9</u>	<u>1.821</u>	<u>0.008</u>	<u>18</u>	<u>1.825-1.817</u>	<u> </u>	<u> </u>
<u>Pu-274</u>	OPTAF	<u>ND</u>	<u> </u>	<u> </u>	<u> </u>	<u> </u>	<u> </u>	<u> </u>

Surface Contamination (g/g)	<u>2.33 × 10⁻¹⁰</u>	Particle Composition	Isotope	Atom %		
Density by	Particle	Coating	Wt % Pu	<u>16.38</u>	<u>Pu-238</u>	<u>0.033</u>
15 psi	<u>2.270</u>	<u>1.801</u>	Wt % Th	<u>NA</u>	<u>Pu-239</u>	<u>88.77</u>
75 psi	<u> </u>	<u> </u>	Wt % U	<u>NA</u>	<u>Pu-240</u>	<u>9.95</u>
10,000 psi	<u>2.315</u>	<u>1.869</u>	Wt % C	<u>45.61</u>	<u>Pu-241</u>	<u>1.144</u>
Defective SiC (fraction):	<u>None</u>		Wt % O	<u>ND</u>	<u>Pu-242</u>	<u>0.107</u>
Missing or incomplete layers (fraction):	<u>1 × 10⁻³</u>		Wt % Si	<u>ND</u>	<u>Pu-244</u>	<u>0.0007</u>
			Other	<u> </u>	<u> </u>	<u> </u>
			Boron Equiv (ppm)	<u> </u>	<u> </u>	<u> </u>
			Iron (ppm)	<u> </u>	<u> </u>	<u> </u>
Coating microstructure and shape:	Accept	<u>X</u>	Reject	<u> </u>	<u> </u>	<u> </u>
Fission gas release R/B:	<u>ND</u>					
Metallographic Data:	Spec. No. <u>P-663</u>	Photo No. <u> </u>	Radiographic Plate No. <u>Pu-274</u>			
Comments:	<u> </u>	<u> </u>	<u> </u>	<u> </u>	<u> </u>	<u> </u>

NA = not applicable ND = not determined. Properties not meeting requirements are circled.

APPENDIX B

Photographs of Coated Particles

This appendix contains photographs of the coated particles, in most cases at 17, 100, 200, and 500 \times magnification. The shapes were determined from the low-magnification photographs, and the microstructures were determined from those at higher magnification.

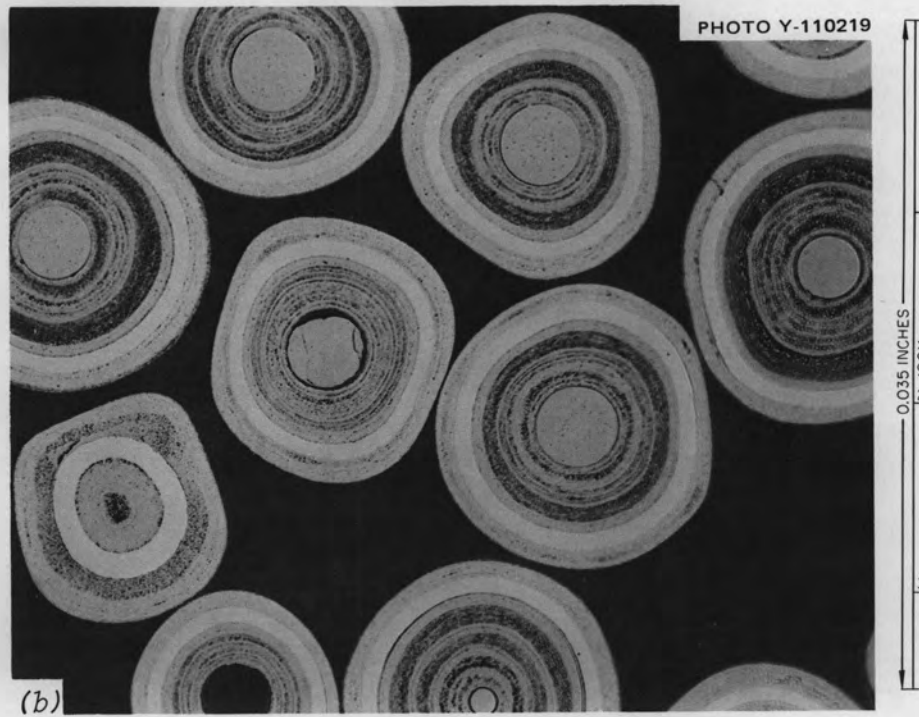
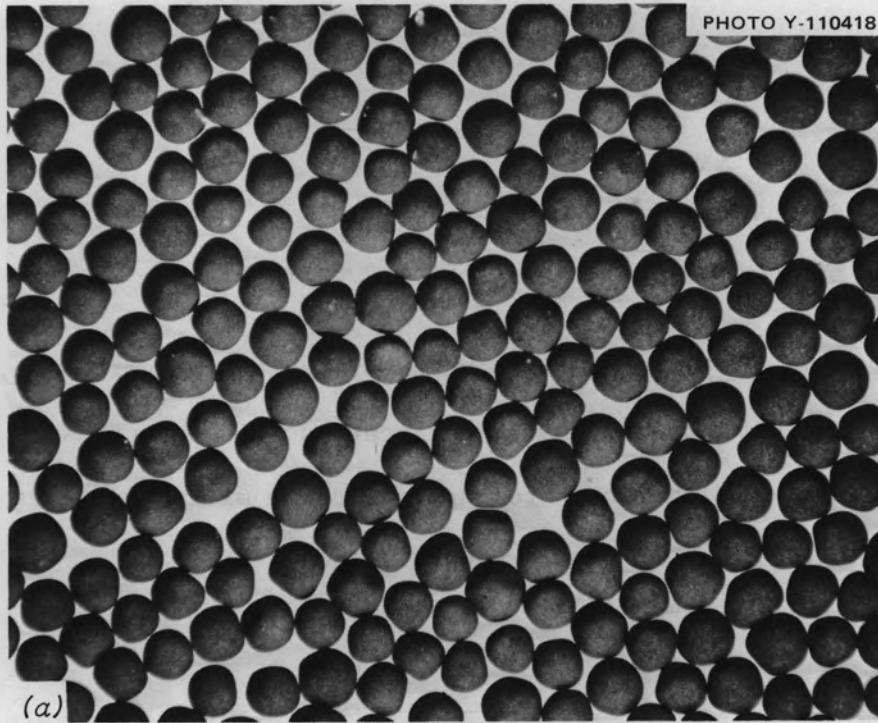


Fig. B-1. Coated particles of type 1. (a) 17x; (b) 100x, bright field.

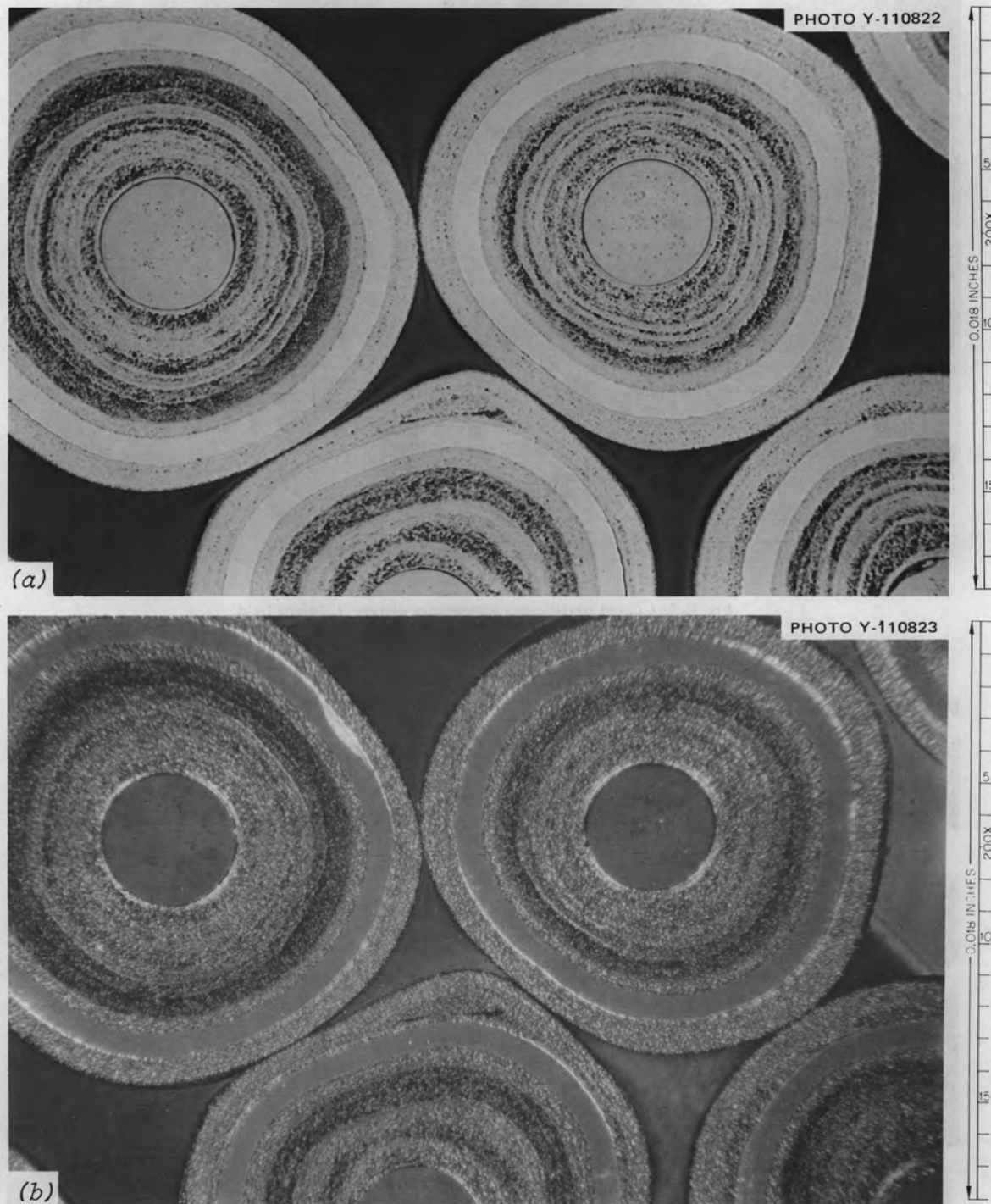


Fig. B-2. Coated particle microstructure of type 1. (a) Bright field; (b) polarized light.

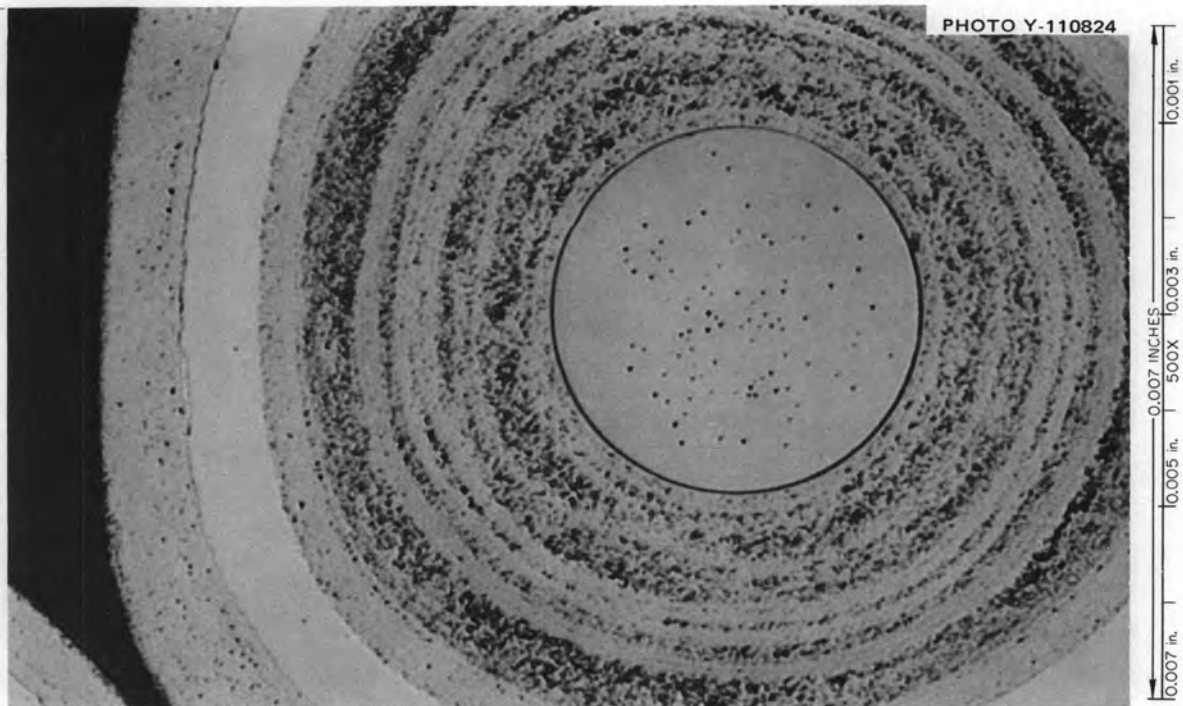


Fig. B-3. Coated particle microstructure of type 1, bright field.

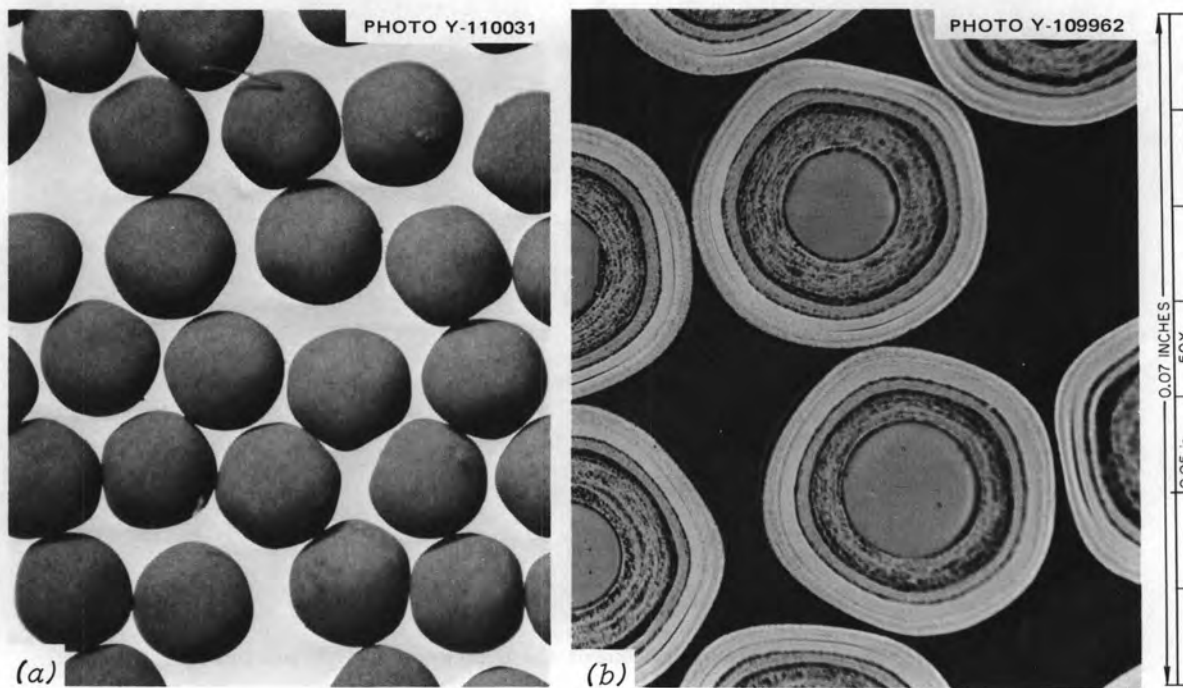


Fig. B-4. Coated particles of type 2. (a) 17X; (b) 50X, bright field.

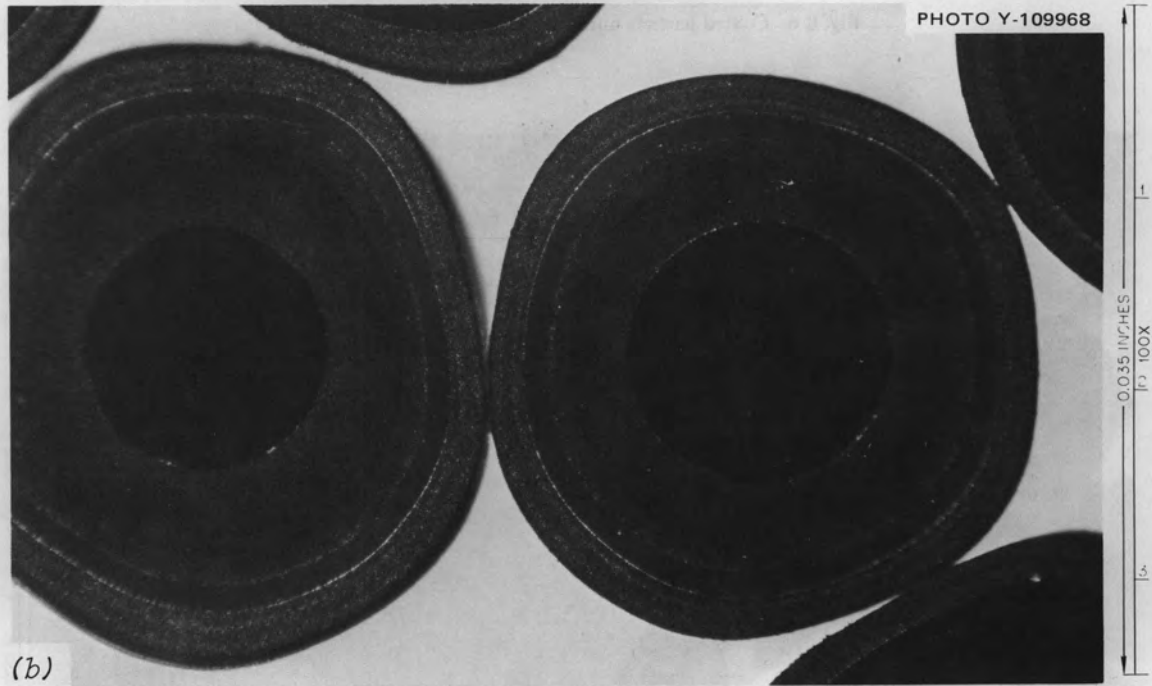
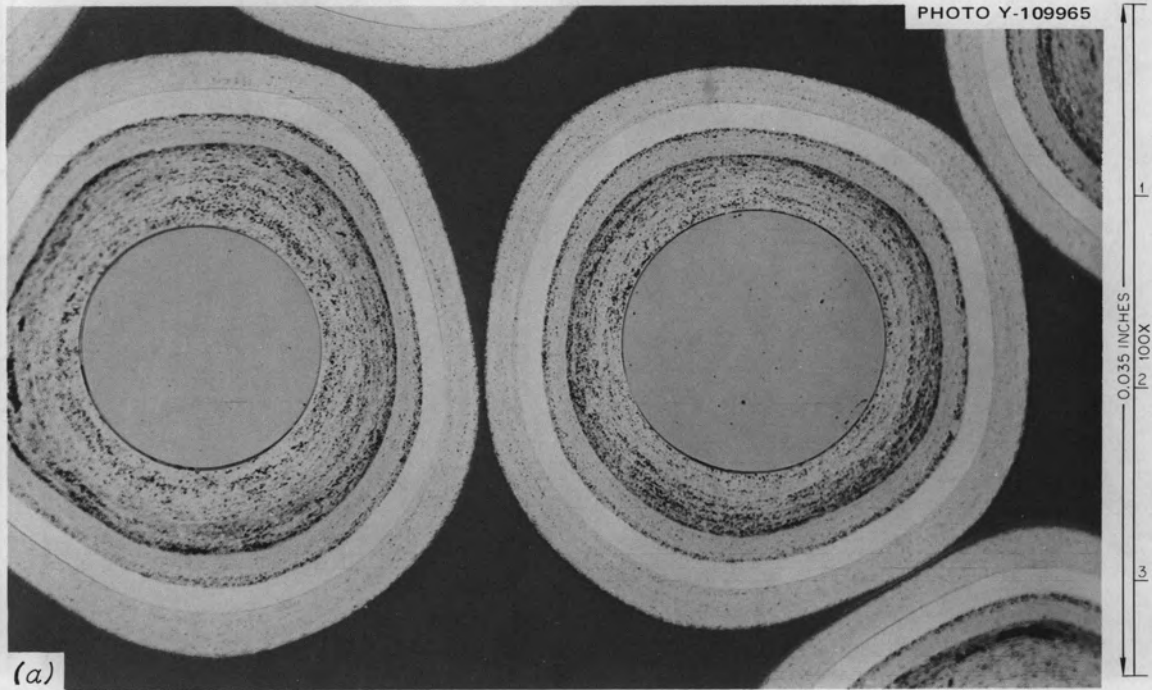


Fig. B-5. Coated particle microstructure of type 2. (a) Bright field; (b) polarized light.

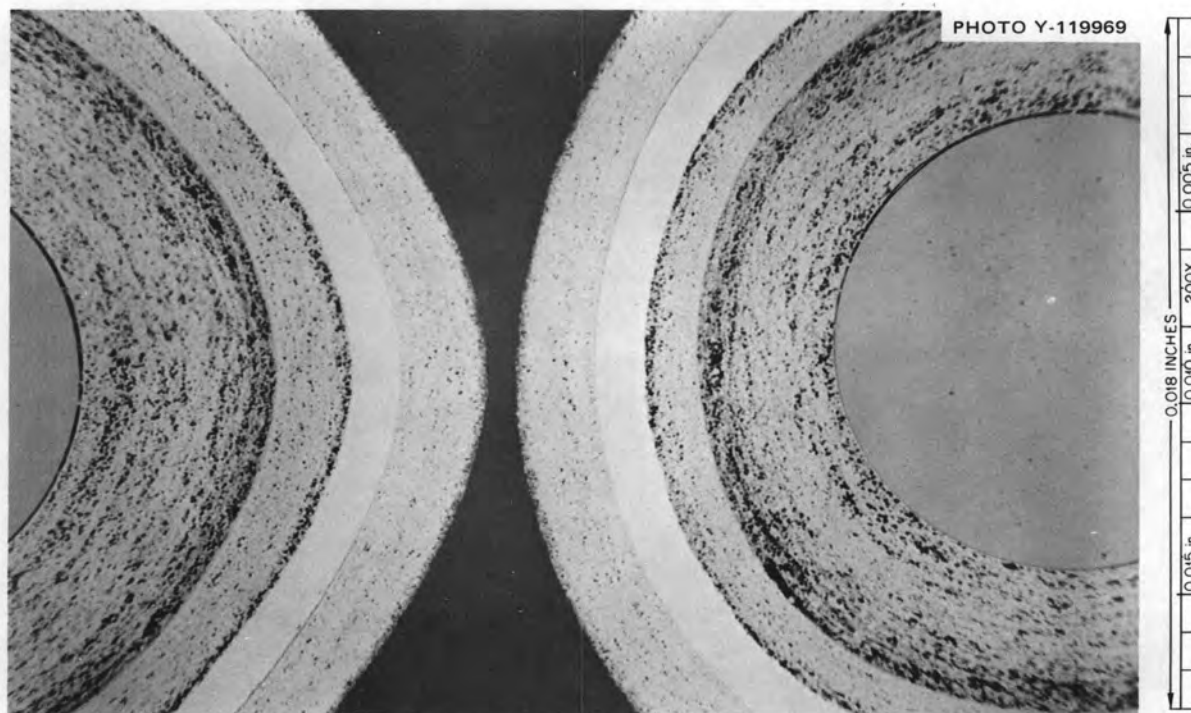


Fig. B-6. Coated particle microstructure of type 2, bright field.

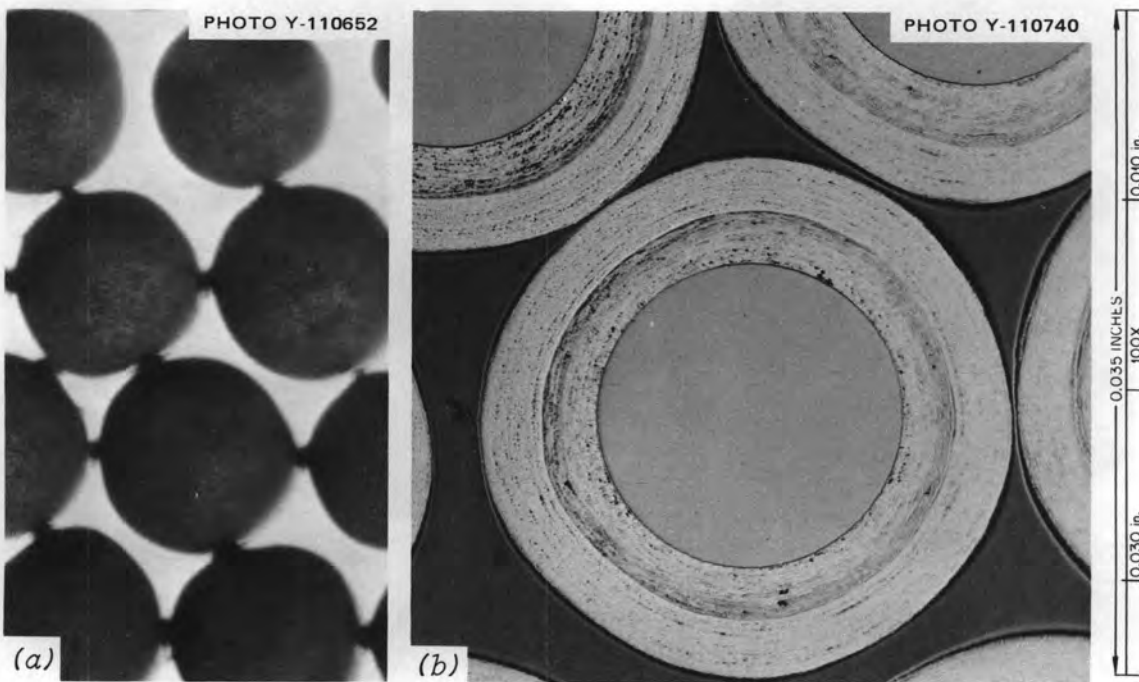


Fig. B-7. Coated particles of type 3. (a) 33X; (b) 100X, bright field.

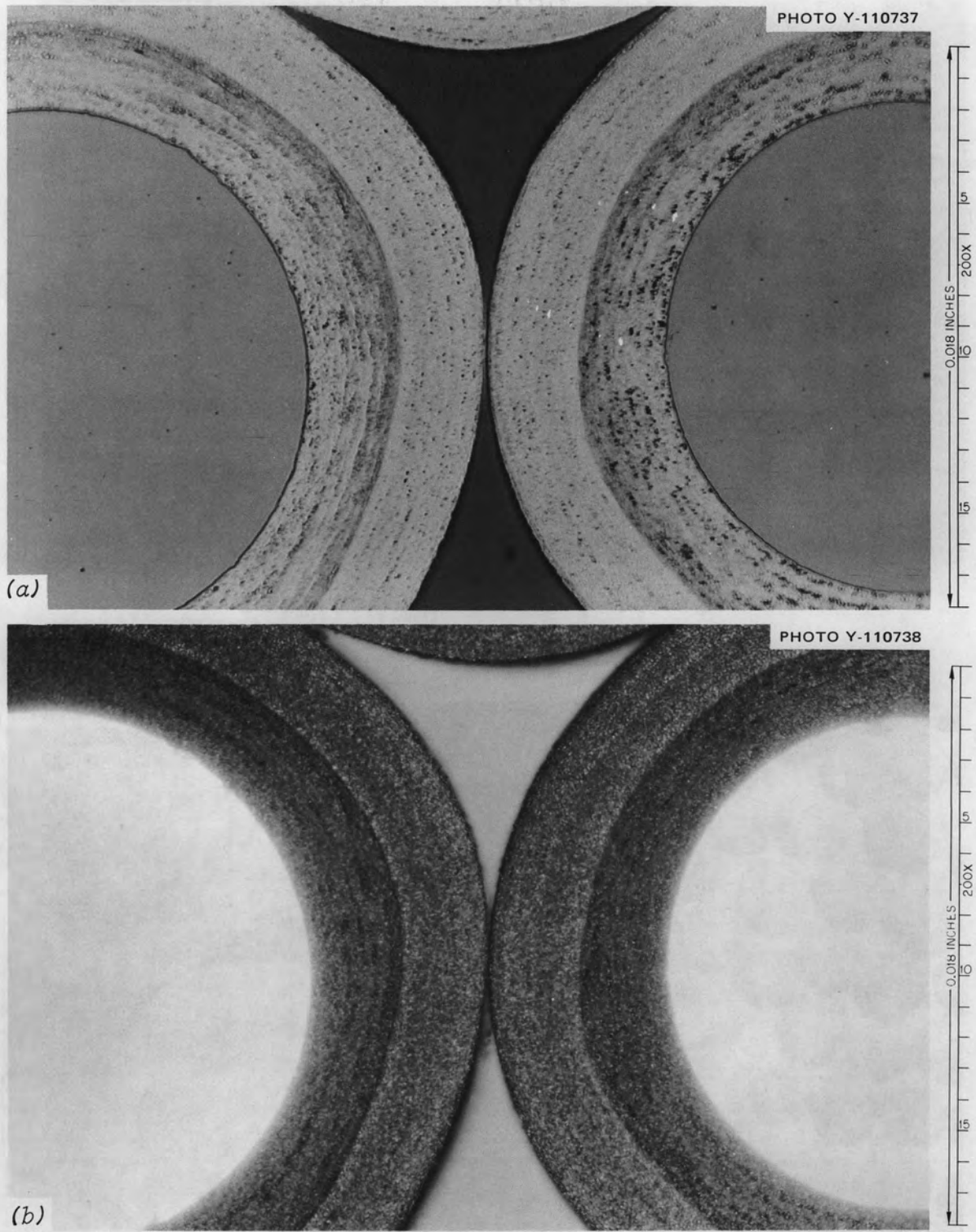


Fig. B-8. Coated particle microstructure of type 3. (a) Bright field; (b) polarized light.

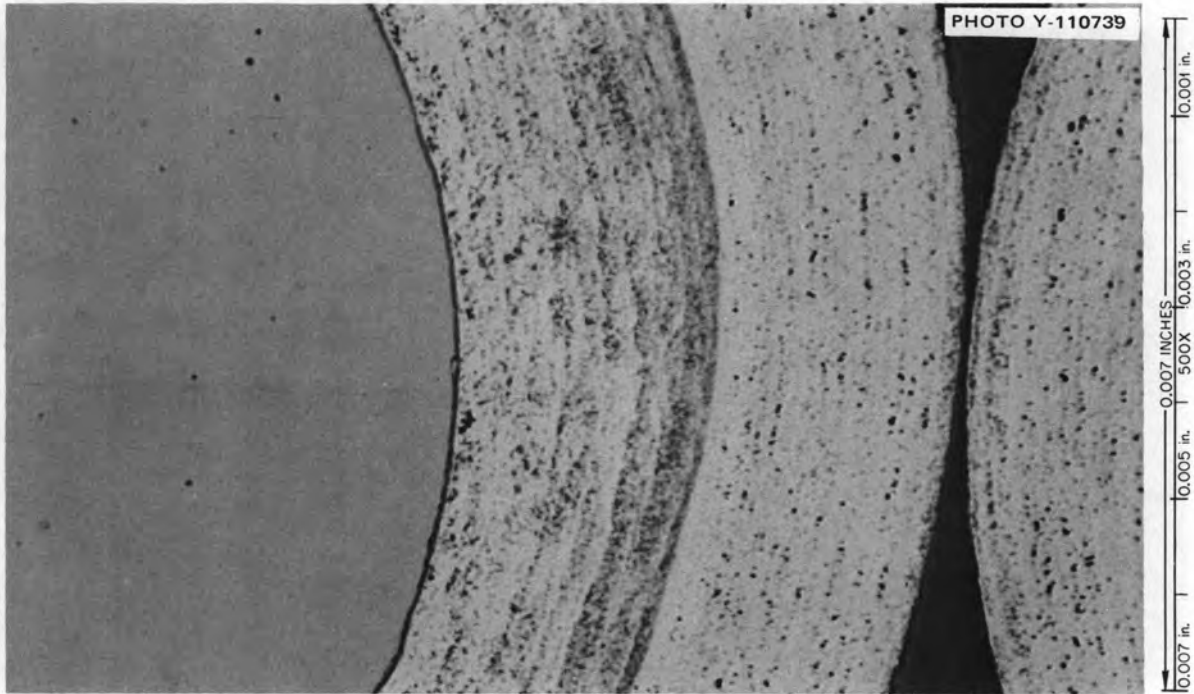


Fig. B-9. Coated particle microstructure of type 3, bright field.

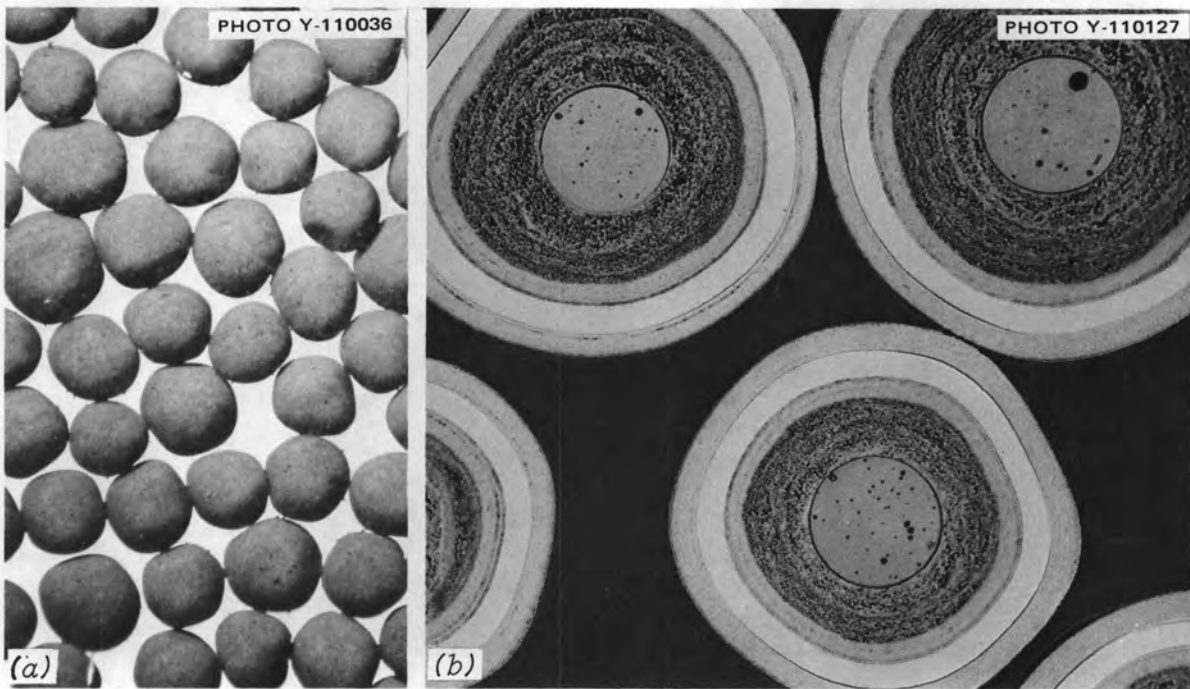


Fig. B-10. Coated particles of type 4. (a) 17X; (b) 100X, bright field.

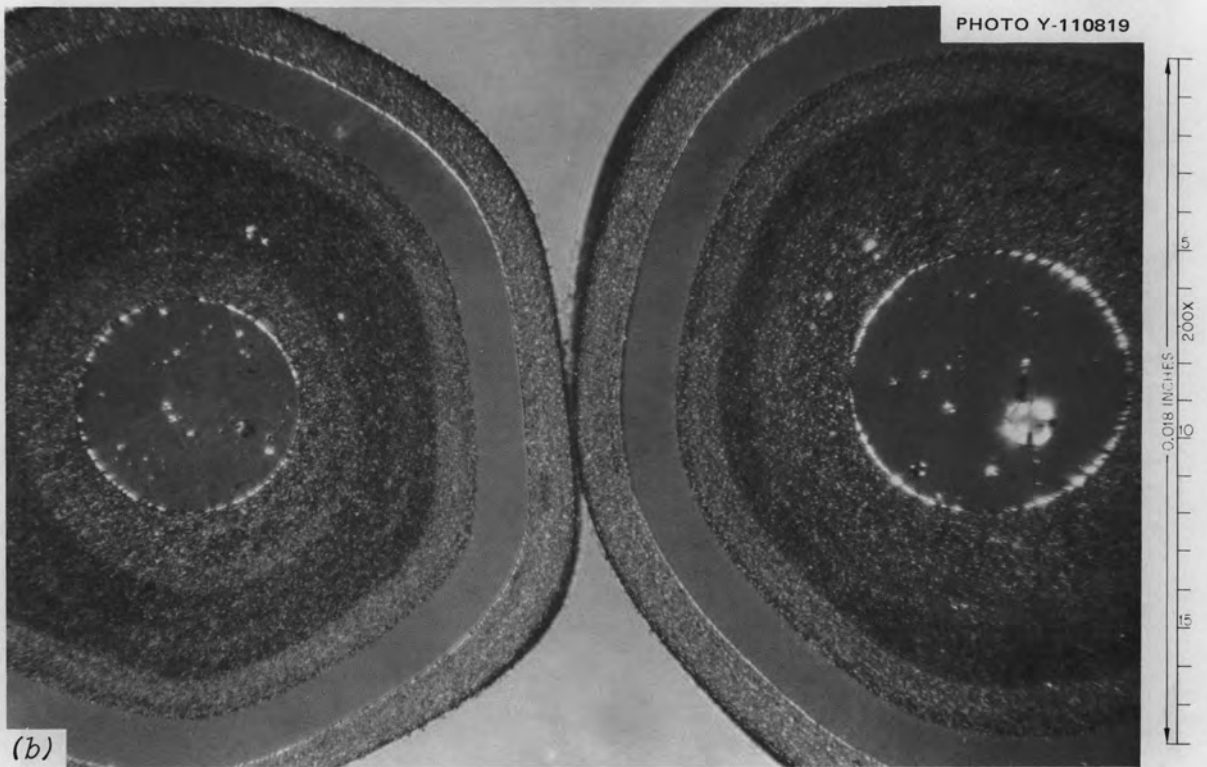
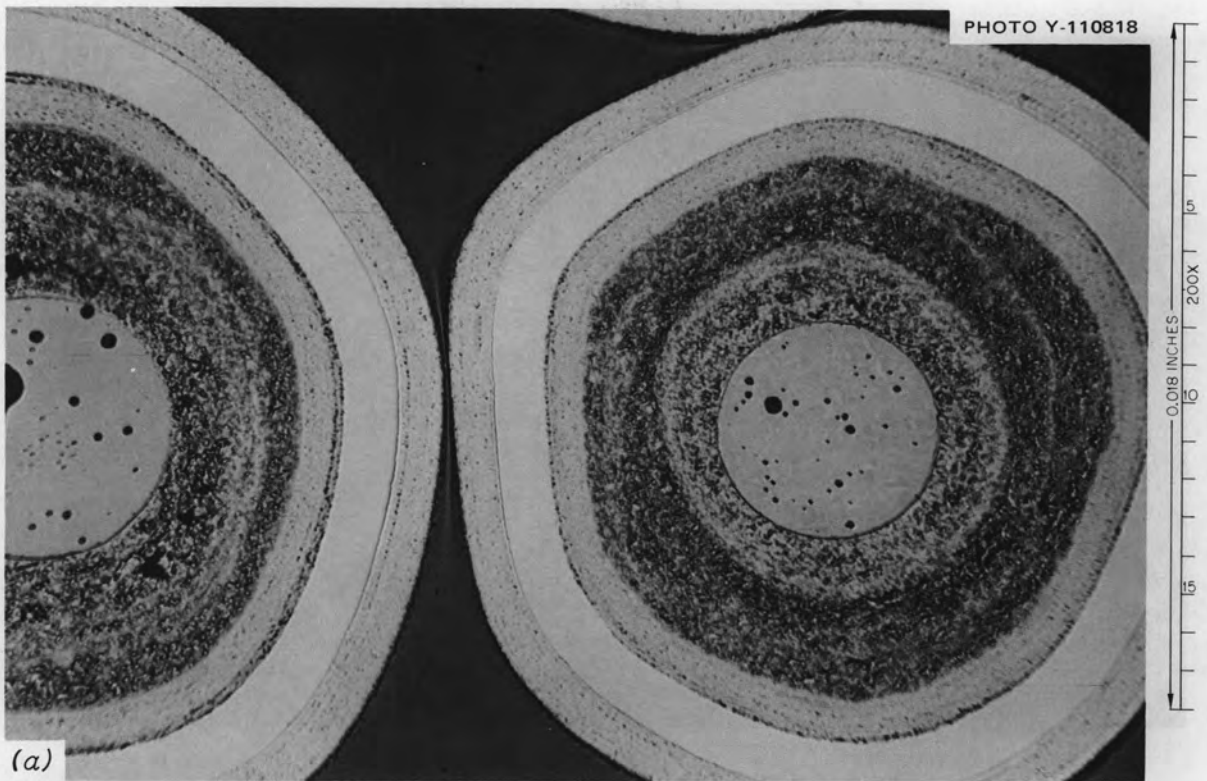


Fig. B-11. Coated particle microstructure of type 4. (a) Bright field; (b) polarized light.

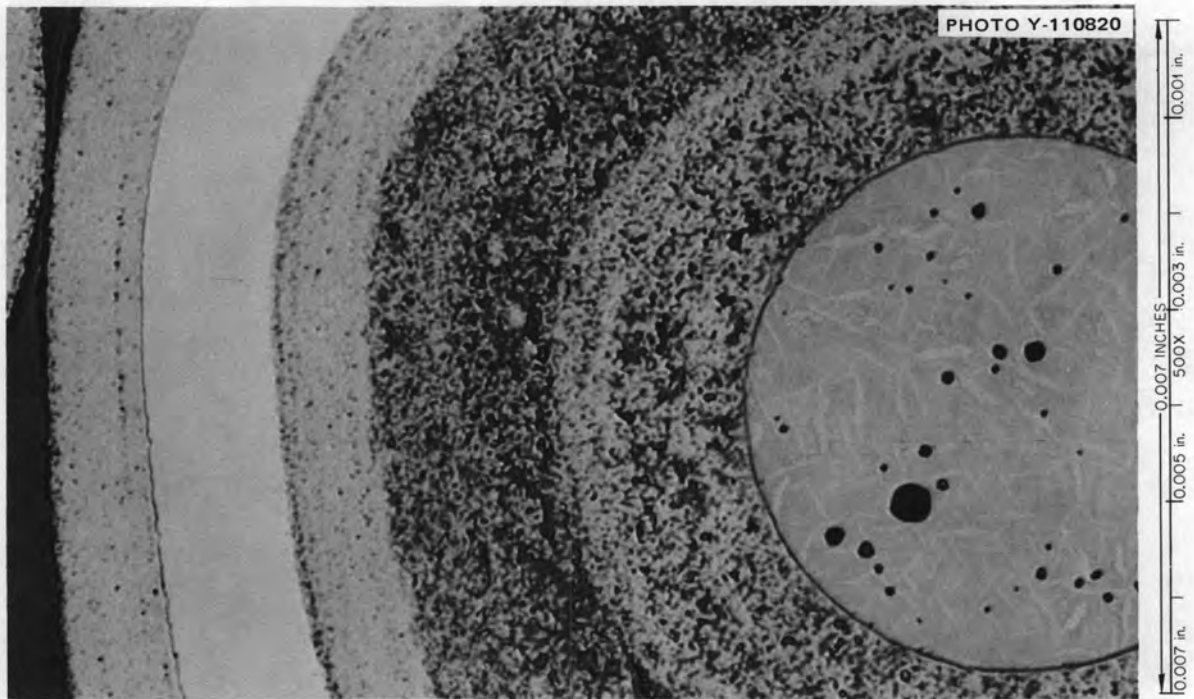


Fig. B-12. Coated particle microstructure of type 4, bright field.

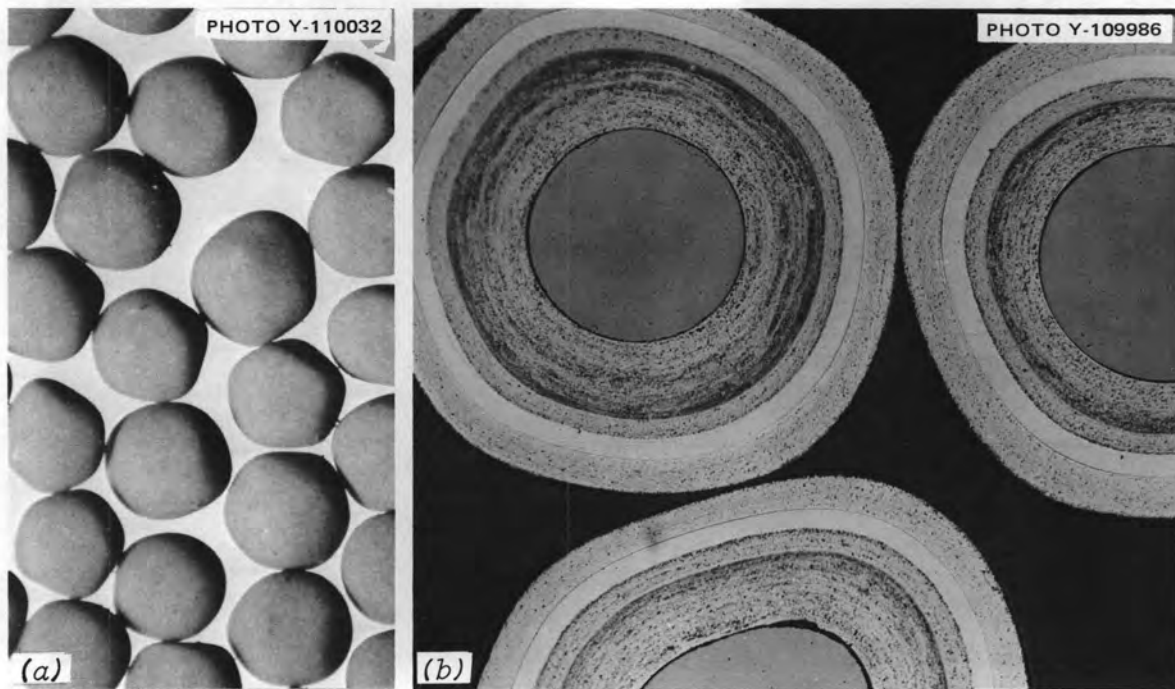


Fig. B-13. Coated particles of type 5. (a) 17X; (b) 100X, bright field.

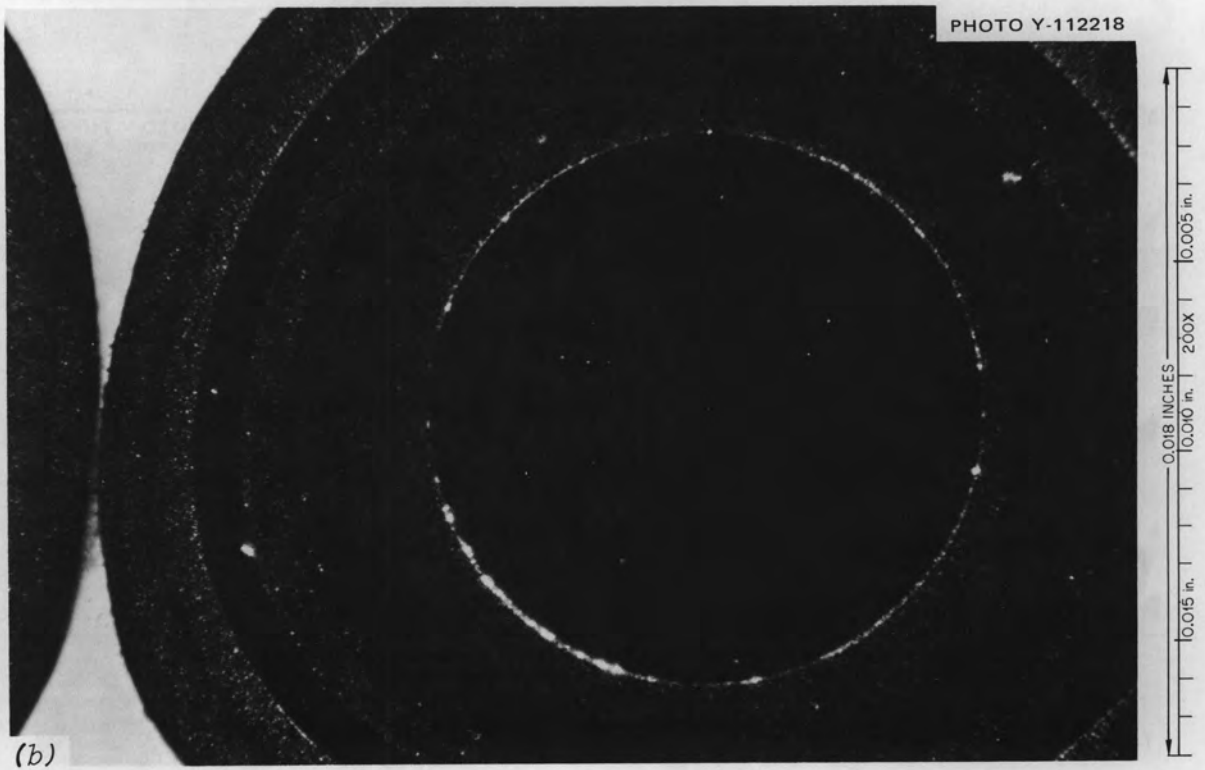
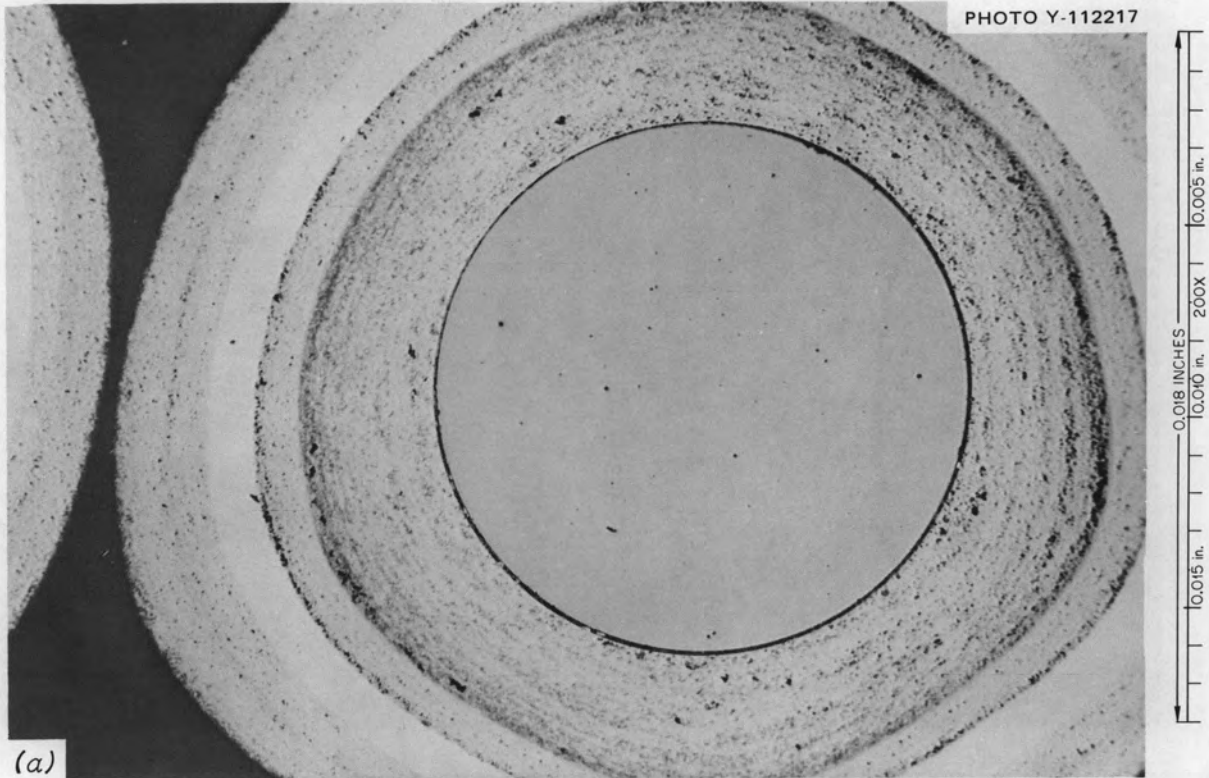


Fig. B-14. Coated particle microstructure of type 5. (a) Bright field; (b) polarized light.

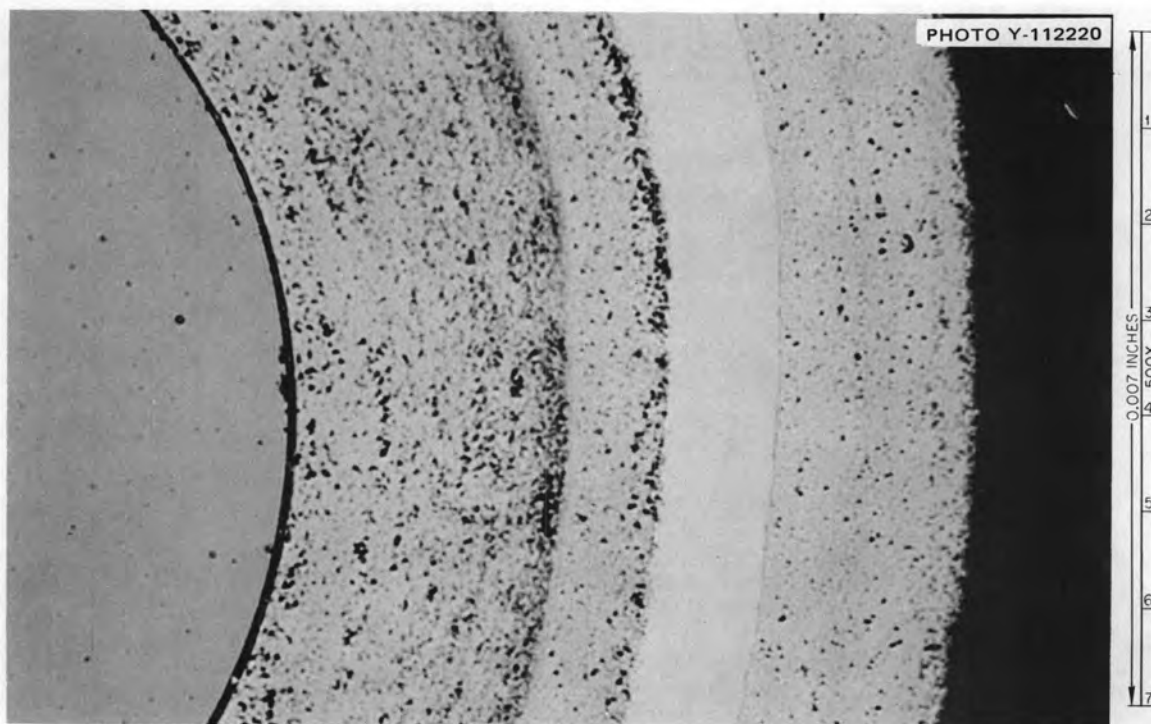


Fig. B-15. Coated particle microstructure of type 5, bright field.

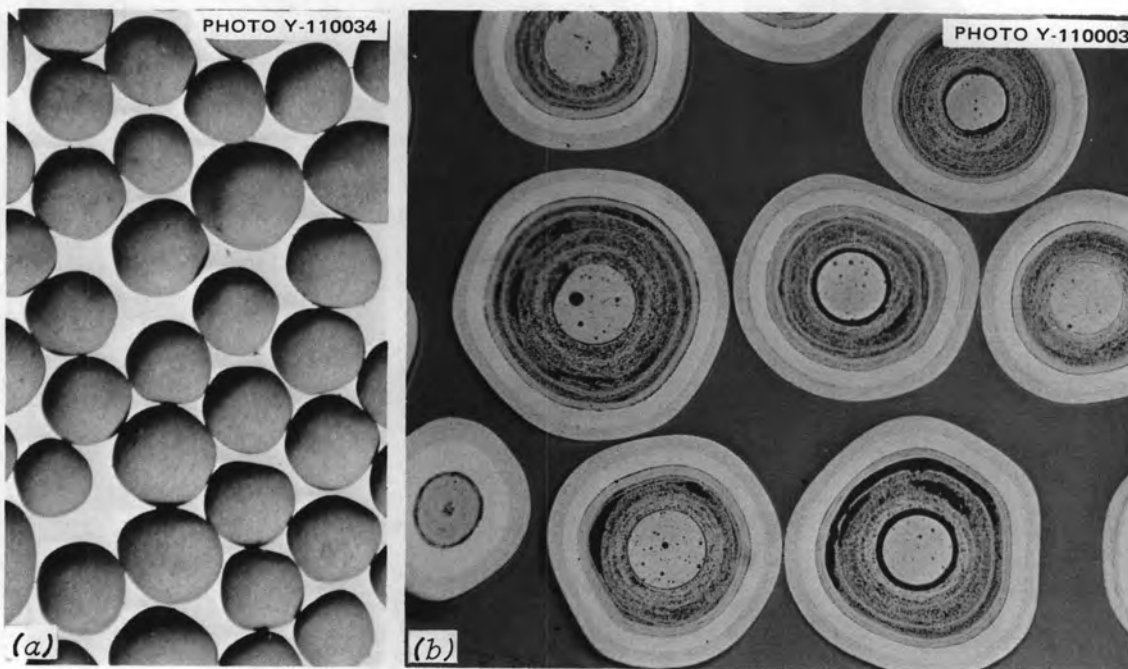


Fig. B-16. Coated particles of type 6. (a) 17 \times ; (b) 50 \times , bright field.

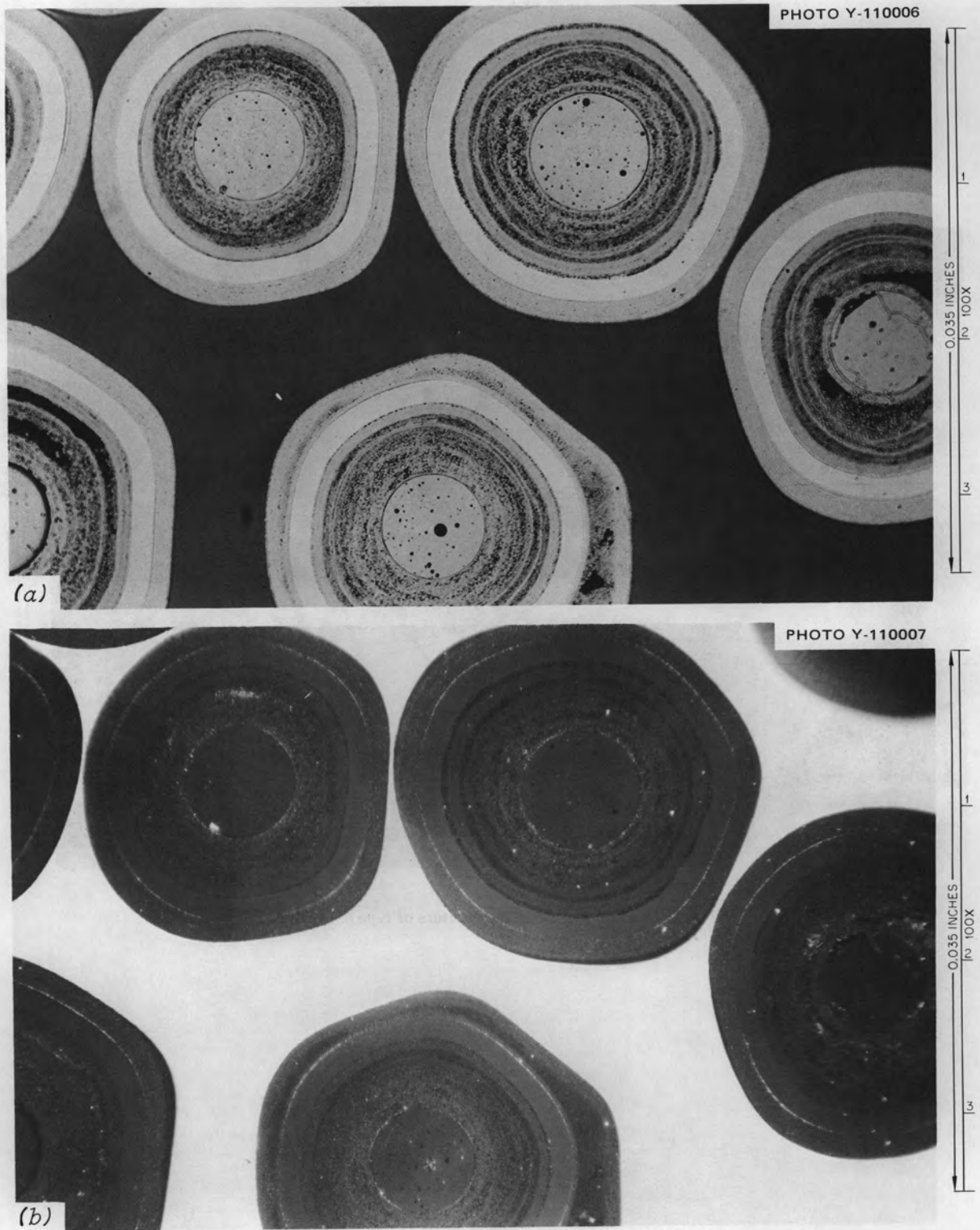


Fig. B-17. Coated particle microstructure of type 6. (a) Bright field; (b) polarized light.

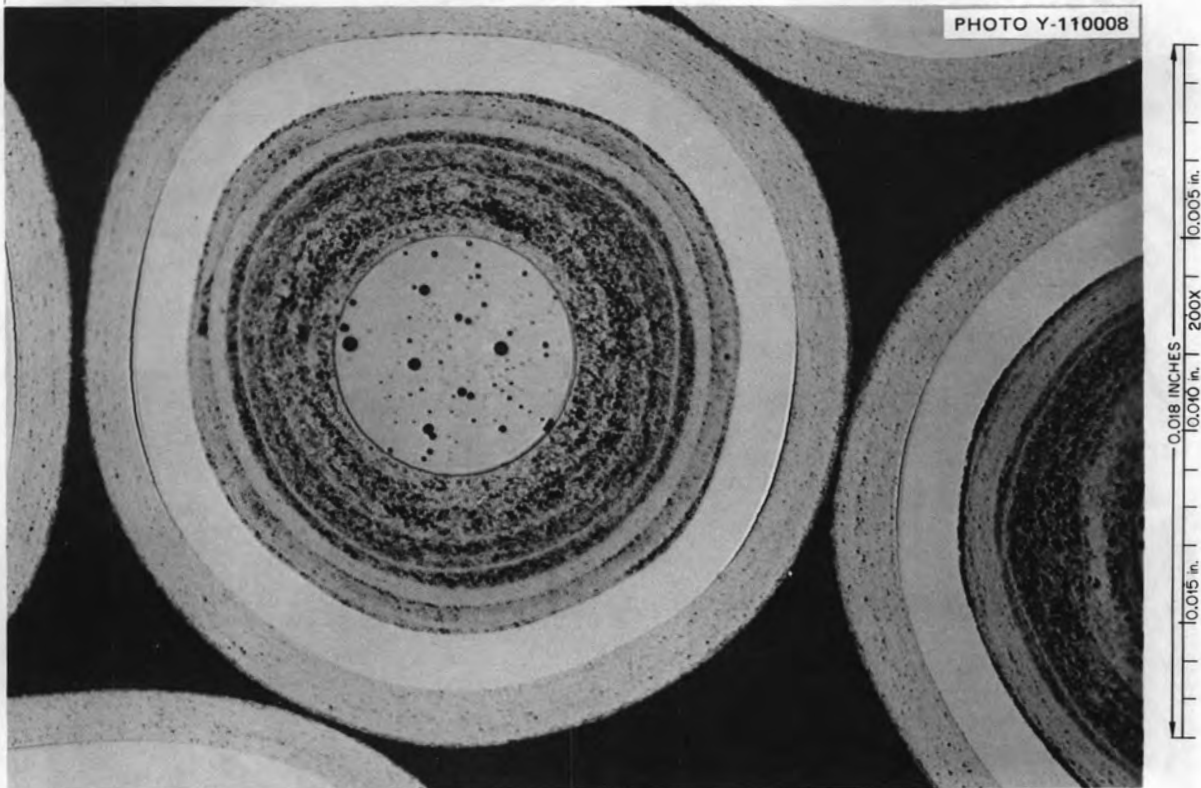


Fig. B-18. Coated particle microstructure of type 6, bright field.

APPENDIX C

Green and Annealed Rod Data

This appendix summarizes the data for the green and annealed rods loaded in the Plutonium Test Element. Each pair of tables give the dimensional and weight data for the loading of one hole in the element.

The average diameter of the annealed rods is based on six measurements, maximum and minimum at each end and the center of the rod. The diameter difference is the difference between the maximum and the minimum of these six measurements.

Hole 1, Fissile Particle Type 5

Green Stick Data and Calculations

Stick Number	Fissile Particle Weight (g)	Fertile Particle Weight (g)	Length (in.)	Weight (g)	Packing Fraction (vol. %)	Matrix Density (g/cm ³)
58108	2	9.478	1.959	14.968	58.6	1.381
58109	1.998	9.478	1.939	14.867	59.19	1.376
58111	2.003	9.478	1.947	14.947	58.98	1.393
58113	2	9.477	1.95	14.979	58.86	1.401
58115	2	9.477	1.95	14.943	58.86	1.387
58118	2	9.477	1.948	14.974	58.92	1.403
58120	2	9.474	1.947	14.961	58.94	1.4
58121	2	9.475	1.944	14.944	59.04	1.398
58122	2	9.476	1.944	14.943	59.04	1.398
58123	2	9.481	1.952	14.973	58.82	1.394
58125	2	9.477	1.961	15.016	58.53	1.397
58126	1.997	9.479	1.942	14.932	59.1	1.397
58127	2.004	9.473	1.944	14.954	59.05	1.402
58129	2.003	9.477	1.955	14.958	58.73	1.384
Diam	0.492					

Annealed Stick Data and Calculations

Stick Number	Length (in.)	Weight (g)	Avg Diam (in.)	Diam Diff. (in.)	Matrix Density (g/cm ³)	Packing Fraction (vol. %)	Coking Value (%)
58108	1.949	12.965	0.4902	0.0005	0.607	59.34	19.7
58109	1.928	12.936	0.4898	0.0005	0.614	60.06	20.4
58111	1.935	12.914	0.4902	0.0005	0.595	59.77	18
58113	1.939	12.968	0.4903	0.0005	0.615	59.6	19.7
58115	1.942	13.032	0.4899	0.001	0.642	59.61	22.9
58118	1.939	13.032	0.4905	0.000	0.64	59.56	22.3
58120	1.94	13.012	0.4902	0.0005	0.635	59.6	21.8
58121	1.932	13.022	0.4902	0.0005	0.644	59.83	22.5
58122	1.936	12.966	0.4902	0.0005	0.618	59.73	20.2
58123	1.942	13.01	0.4902	0.0005	0.629	59.55	21.4
58125	1.946	13.05	0.49	0.001	0.645	59.47	22.3
58126	1.933	13.005	0.4901	0.0005	0.637	59.84	22
58127	1.935	12.98	0.4902	0.0005	0.624	59.75	20.6
58129	1.943	12.98	0.4902	0.0005	0.617	59.54	20.5

Hole 2, Fissile Particle Type 6

Green Stick Data and Calculations

Stick Number	Fissile Particle Weight (g)	Fertile Particle Weight (g)	Length (in.)	Weight (g)	Packing Fraction (vol. %)	Matrix Density (g/cm ³)
58177	1.079	10.461	1.955	14.95	60.8	1.428
58179	1.079	10.47	1.94	14.953	61.32	1.456
58180	1.079	10.463	1.956	14.997	60.78	1.446
58181	1.079	10.466	1.954	14.99	60.86	1.446
58184	1.084	10.468	1.94	15.027	61.35	1.488
58186	1.079	10.464	1.946	15	61.1	1.466
58187	1.079	10.466	1.959	15.047	60.7	1.46
58188	1.079	10.465	1.945	14.99	61.13	1.463
58189	1.08	10.464	1.933	14.923	61.52	1.458
58190	1.081	10.467	1.94	15.002	61.32	1.477
58191	1.079	10.468	1.951	15.025	60.96	1.466
58192	1.083	10.463	1.932	14.965	61.57	1.478
58194	1.079	10.463	1.944	14.97	61.16	1.457
58195	1.079	10.469	1.93	14.939	61.63	1.47
Diam	0.492					

Annealed Stick Data and Calculations

Stick Number	Length (in.)	Weight (g)	Avg Diam (in.)	Diam Diff. (in.)	Matrix Density (g/cm ³)	Packing Fraction (vol. %)	Coking Value (%)
58177	1.945	13	0.4899	0.0013	0.633	61.63	20
58179	1.925	13.032	0.4902	0.001	0.66	62.26	21.1
58180	1.943	13.077	0.4904	0.0013	0.665	61.59	22.3
58181	1.946	12.99	0.4898	0.001	0.627	61.65	18.8
58184	1.929	13.04	0.4896	0.0015	0.663	62.31	20
58186	1.939	13.05	0.4901	0.001	0.658	61.8	21.1
58187	1.952	12.953	0.4892	0.0015	0.61	61.61	16.4
58188	1.925	13.022	0.4897	0.001	0.661	62.36	20.1
58189	1.922	12.98	0.4897	0.001	0.644	62.44	19.6
58190	1.928	12.992	0.4898	0.0005	0.642	62.25	18.6
58191	1.945	13.013	0.4897	0.001	0.638	61.71	19.1
58192	1.937	13.05	0.4902	0.0005	0.659	61.87	21.7
58194	1.932	13.066	0.4904	0.001	0.669	61.93	22.3
58195	1.923	12.999	0.4898	0.001	0.65	62.4	20

Hole 3, Fissile Particle Type 6

Green Stick Data and Calculations

Stick Number	Fissile Particle Weight (g)	Fertile Particle Weight (g)	Length (in.)	Weight (g)	Packing Fraction (vol. %)	Matrix Density (g/cm ³)
58199	1.079	10.468	1.946	14.993	61.12	1.462
58200	1.08	10.468	1.941	14.988	61.28	1.469
58201	1.079	10.464	1.946	15.003	61.1	1.467
58202	1.079	10.467	1.938	14.969	61.36	1.467
58204	1.079	10.47	1.953	15.024	60.91	1.461
58208	1.084	10.463	1.964	15.029	60.58	1.444
58209	1.079	10.468	1.932	14.96	61.56	1.475
58210	1.079	10.469	1.964	15.056	60.56	1.454
58211	1.079	10.467	1.952	15.002	60.92	1.454
58213	1.079	10.47	1.937	14.952	61.41	1.461
58214	1.081	10.463	1.948	15.012	61.05	1.467
58215	1.079	10.464	1.938	14.957	61.35	1.463
58216	1.084	10.467	1.957	15.045	60.81	1.462
58217	1.079	10.469	1.927	14.926	61.72	1.47
Diam	0.492					

Annealed Stick Data and Calculations

Stick Number	Length (in.)	Weight (g)	Avg Diam (in.)	Diam Diff. (in.)	Matrix Density (g/cm ³)	Packing Fraction (vol. %)	Coking Value (%)
58199	1.934	13.035	0.4892	0.0005	0.661	62.19	20.5
58200	1.929	13.031	0.4896	0.001	0.661	62.27	20.4
58201	1.938	13.05	0.4898	0.001	0.661	61.89	21.1
58202	1.928	13.057	0.49	0.001	0.671	62.19	21.9
58204	1.939	13.073	0.4902	0.0015	0.665	61.79	21.5
58208	1.952	13.117	0.4898	0.001	0.676	61.49	23.2
58209	1.92	13.019	0.4897	0.0015	0.663	62.54	20.5
58210	1.957	13.083	0.4902	0.0005	0.654	61.23	21.3
58211	1.939	13.11	0.4897	0.0005	0.686	61.9	23.4
58213	1.92	13.037	0.4902	0.0005	0.667	62.42	21.3
58214	1.939	13.082	0.4902	0.0005	0.671	61.77	22.2
58215	1.93	13.031	0.4902	0.0005	0.657	62.04	21.1
58216	1.946	13.087	0.4903	0.001	0.664	61.57	21.6
58217	1.916	13.033	0.4902	0.0005	0.669	62.52	21.6

Hole 4, Fissile Particle Type 1

Green Stick Data and Calculations

Stick Number	Fissile Particle Weight (g)	Fertile Particle Weight (g)	Length (in.)	Weight (g)	Packing Fraction (vol. %)	Matrix Density (g/cm ³)
58222	1.633	9.963	1.955	14.926	60.7	1.391
58223	1.633	9.969	1.948	14.94	60.94	1.408
58224	1.628	9.965	1.936	14.906	61.26	1.418
58225	1.628	9.965	1.951	14.927	60.79	1.399
58226	1.628	9.962	1.926	14.859	61.57	1.418
58227	1.628	9.962	1.925	14.885	61.6	1.431
58228	1.628	9.966	1.971	15.059	60.13	1.417
58229	1.628	9.966	1.934	14.894	61.33	1.416
58230	1.628	9.966	1.921	14.898	61.75	1.443
58231	1.628	9.964	1.93	14.88	61.45	1.418
58235	1.628	9.962	1.919	14.857	61.79	1.43
58239	1.628	9.964	1.945	14.911	60.98	1.404
58240	1.628	9.964	1.944	14.92	61.01	1.409
58241	1.628	9.964	1.95	14.952	60.82	1.412
Diam	0.492					

Annealed Stick Data and Calculations

Stick Number	Length (in.)	Weight (g)	Avg Diam (in.)	Diam Diff. (in.)	Matrix Density (g/cm ³)	Packing Fraction (vol. %)	Coking Value (%)
58222	1.948	13.087	0.4909	0.001	0.636	61.18	22.8
58223	1.935	13.14	0.4907	0.0015	0.669	61.67	24.6
58224	1.924	13.074	0.4907	0.0005	0.653	61.96	22.7
58225	1.932	13.096	0.4905	0.001	0.657	61.77	23.2
58226	1.916	13.049	0.4908	0.0005	0.649	62.18	22.6
58227	1.913	13.09	0.4909	0.0005	0.67	62.26	23.8
58228	1.958	13.152	0.4903	0.001	0.659	60.99	23
58229	1.923	13.098	0.4908	0.0005	0.663	61.98	23.9
58230	1.91	13.098	0.4909	0.001	0.675	62.38	23.8
58231	1.917	13.054	0.4906	0.0005	0.652	62.22	22.3
58235	1.913	13.044	0.4904	0.0005	0.653	62.39	22.4
58239	1.93	13.003	0.4906	0.0005	0.618	61.8	19.6
58240	1.925	13.04	0.4911	0.0005	0.635	61.84	21
58241	1.943	13.12	0.4907	0.0005	0.656	61.35	23.7

Hole 5, Fissile Particle Type 1

Green Stick Data and Calculations

Stick Number	Fissile Particle Weight (g)	Fertile Particle Weight (g)	Length (in.)	Weight (g)	Packing Fraction (vol. %)	Matrix Density (g/cm ³)
58245	1.628	9.965	1.943	14.914	61.04	1.408
58246	1.628	9.962	1.931	14.863	61.41	1.41
58247	1.63	9.963	1.965	14.97	60.36	1.392
58248	1.628	9.963	1.945	14.923	60.97	1.409
58249	1.628	9.963	1.945	14.933	60.97	1.413
58250	1.628	9.963	1.945	14.955	60.97	1.422
58253	1.628	9.964	1.936	14.919	61.26	1.424
58255	1.629	9.965	1.937	14.912	61.24	1.419
58258	1.628	9.966	1.924	14.904	61.65	1.44
58260	1.628	9.966	1.947	14.928	60.92	1.407
58261	1.628	9.966	1.932	14.942	61.4	1.441
58262	1.628	9.967	1.934	14.924	61.34	1.429
58263	1.628	9.967	1.931	14.917	61.43	1.432
58264	1.628	9.967	1.938	14.905	61.21	1.413
Diam	0.492					

Annealed Stick Data and Calculations

Stick Number	Length (in.)	Weight (g)	Avg Diam (in.)	Diam Diff. (in.)	Matrix Density (g/cm ³)	Packing Fraction (vol. %)	Coking Value (%)
58245	1.93	13.129	0.4903	0.0005	0.675	61.89	24.8
58246	1.919	13.073	0.491	0.001	0.656	62.04	23.5
58247	1.952	13.14	0.491	0.001	0.655	61.01	24.2
58248	1.932	13.113	0.4906	0.0005	0.665	61.74	24
58249	1.934	13.106	0.4912	0.0005	0.656	61.53	23.5
58250	1.935	13.118	0.491	0.001	0.661	61.54	23.6
58253	1.924	13.103	0.4909	0.0005	0.665	61.91	23.7
58255	1.922	13.109	0.4905	0.001	0.672	62.1	24
58258	1.913	13.092	0.4911	0.001	0.668	62.24	23.4
58260	1.937	13.051	0.491	0.001	0.629	61.49	21.3
58261	1.943	13.08	0.4908	0.0005	0.639	61.36	22.2
58262	1.922	13.082	0.4913	0.0005	0.653	61.89	22.6
58263	1.92	13.075	0.4908	0.001	0.656	62.08	22.4
58264	1.931	13.097	0.4911	0.001	0.654	61.66	23.6

Hole 6, Fissile Particle Type 4
Green Stick Data and Calculations

Stick Number	Fissile Particle Weight (g)	Fertile Particle Weight (g)	Length (in.)	Weight (g)	Packing Fraction (vol. %)	Matrix Density (g/cm ³)
58150	1.002	10.404	1.934	14.84	59.5	1.407
58151	1.001	10.402	1.928	14.836	59.67	1.417
58152	1.004	10.405	1.932	14.813	59.59	1.399
58153	1.01	10.339	1.935	14.812	59.22	1.409
58154	1	10.503	1.929	14.893	60.13	1.415
58155	1.002	10.496	1.932	14.957	60.02	1.437
58157	1	10.506	1.947	14.941	59.59	1.401
58159	1.005	10.505	1.948	14.963	59.59	1.408
58160	1.003	10.498	1.933	14.904	60.01	1.413
58164	0.998	10.5	1.938	14.926	59.82	1.413
58167	1.003	10.5	1.936	14.892	59.92	1.402
58169	0.999	10.502	1.932	14.963	60.02	1.439
58170	1.002	10.5	1.931	14.911	60.07	1.419
58171	0.998	10.495	1.94	14.923	59.73	1.409
Diam	0.492					

Annealed Stick Data and Calculations

Stick Number	Length (in.)	Weight (g)	Avg Diam (in.)	Diam Diff. (in.)	Matrix Density (g/cm ³)	Packing Fraction (vol. %)	Coking Value (%)
58150	1.927	12.83	0.4898	0.001	0.602	60.25	18.1
58151	1.919	12.843	0.49	0.001	0.614	60.44	18.8
58152	1.922	12.862	0.49	0.000	0.618	60.39	19.8
58153	1.942	12.823	0.49	0.001	0.606	59.49	19.7
58154	1.916	13.007	0.4904	0.001	0.649	60.93	22.2
58155	1.929	12.909	0.4898	0.001	0.602	60.64	17.2
58157	1.931	12.914	0.4896	0.001	0.601	60.68	17.5
58159	1.935	12.994	0.4902	0.0005	0.627	60.44	20.2
58160	1.918	13	0.4902	0.0005	0.646	60.91	21.7
58164	1.925	12.977	0.4901	0.001	0.632	60.69	20.5
58167	1.922	13.023	0.4906	0.001	0.65	60.71	22.9
58169	1.922	12.916	0.4895	0.001	0.611	60.95	17.3
58170	1.919	12.968	0.4907	0.0005	0.629	60.77	20.3
58171	1.928	12.961	0.4899	9.0005	0.626	60.62	20

Hole 7, Fissile Particle Type 2

Green Stick Data and Calculations

Stick Number	Fissile Particle Weight (g)	Fertile Particle Weight (g)	Length (in.)	Weight (g)	Packing Fraction (vol. %)	Matrix Density (g/cm ³)
5877	2.14	9.34	2.013	15.076	57.53	1.35
5879	2.138	9.053	1.928	14.588	58.64	1.367
5880	2.132	9.066	1.933	14.684	58.51	1.395
5882	2.137	9.059	1.942	14.686	58.24	1.381
5883	2.137	9.2	1.942	14.723	58.93	1.363
5884	2.14	9.204	1.938	14.82	59.09	1.407
5890	2.138	9.199	1.936	14.82	59.11	1.412
5891	2.138	9.203	1.935	14.767	59.16	1.392
5894	2.137	9.194	1.961	14.848	58.33	1.381
5895	2.137	9.2	1.91	14.688	59.92	1.405
5896	2.134	9.197	1.922	14.746	59.51	1.408
5897	2.139	9.197	1.942	14.755	58.93	1.376
5899	2.136	9.199	1.929	14.74	59.32	1.393
58100	2.134	9.2	1.94	14.789	58.97	1.393
Diam	0.492					

Annealed Stick Data and Calculations

Stick Number	Length (in.)	Weight (g)	Avg Diam (in.)	Diam Diff. (in.)	Matrix Density (g/cm ³)	Packing Fraction (vol. %)	Coking Value (%)
5877	2.001	12.878	0.489	0.000	0.548	58.59	14.5
5879	1.915	12.621	0.49	0.001	0.595	59.44	19
5880	1.923	12.612	0.491	0.001	0.577	58.98	16.9
5882	1.929	12.618	0.49	0.001	0.581	59.03	17.1
5883	1.93	12.76	0.49	0.000	0.593	59.78	18.9
5884	1.929	12.712	0.49	0.000	0.572	59.85	15.2
5890	1.926	12.75	0.49	0.001	0.59	59.83	16.9
5891	1.924	12.742	0.49	0.001	0.587	59.91	17.3
5894	1.953	12.808	0.491	0.000	0.592	58.81	18.9
5895	1.9	12.706	0.49	0.001	0.592	60.64	17.3
5896	1.914	12.745	0.49	0.000	0.601	60.25	18
5897	1.925	12.794	0.49	0.001	0.61	59.85	19.8
5899	1.918	12.762	0.49	0.000	0.604	60.14	18.8
58100	1.925	12.752	0.491	0.001	0.591	59.75	17.5

Hole 8, Fissile Particle Type 5

Green Stick Data and Calculations

Stick Number	Fissile Particle Weight (g)	Fertile Particle Weight (g)	Length (in.)	Weight (g)	Packing Fraction (vol. %)	Matrix Density (g/cm ³)
58131	2.005	9.479	1.939	14.909	59.24	1.391
58132	2.005	9.476	1.945	14.92	59.04	1.386
58134	2	9.475	1.948	14.922	58.91	1.382
58135	1.999	9.475	1.942	14.897	59.09	1.383
58136	2.005	9.477	1.952	14.972	58.84	1.394
58137	1.999	9.477	1.945	14.941	59.01	1.395
58138	2	9.475	1.957	14.955	58.64	1.38
58139	1.995	9.474	1.963	14.985	58.43	1.383
58140	2	9.48	1.956	14.946	58.7	1.377
58141	2.004	9.482	1.966	14.971	58.43	1.369
58142	2.002	9.48	1.95	14.951	58.89	1.389
58143	2	9.479	1.949	14.96	58.9	1.395
58144	2.005	9.48	1.939	14.937	59.24	1.402
58147	1.998	9.477	1.977	14.955	58.05	1.347
Diam	0.492					

Annealed Stick Data and Calculations

Stick Number	Length (in.)	Weight (g)	Avg Diam (in.)	Diam Diff. (in.)	Matrix Density (g/cm ³)	Packing Fraction (vol. %)	Coking Value (%)
58131	1.926	13.037	0.4901	0.001	0.654	60.11	23.6
58132	1.929	13.041	0.4905	0.001	0.651	59.9	23.6
58134	1.934	13.013	0.4897	0.002	0.642	59.89	22.5
58135	1.927	13.002	0.4902	0.001	0.64	59.98	22.6
58136	1.941	12.976	0.4899	0.001	0.618	59.67	20
58137	1.932	13.024	0.4903	0.0015	0.644	59.81	22.6
58138	1.948	13.04	0.4902	0.0015	0.639	59.34	23
58139	1.952	13	0.49	0.001	0.623	59.24	21
58140	1.946	13.049	0.4904	0.001	0.641	59.38	23.5
58141	1.95	12.992	0.4899	0.001	0.616	59.42	20.6
58142	1.939	13.037	0.49	0.001	0.644	59.71	22.8
58143	1.94	12.998	0.4901	0.001	0.628	59.64	21.2
58144	1.929	12.969	0.4901	0.0015	0.622	60.02	20.3
58147	1.957	13.034	0.4903	0.001	0.629	59.04	22.8



APPENDIX D

Photographs of Microstructure of Rods

This appendix contains photographs originally at 40, 250, and 750× of the microstructure of one fuel rod with each fissile particle type.

ITEM 1

PHOTO Y-112239

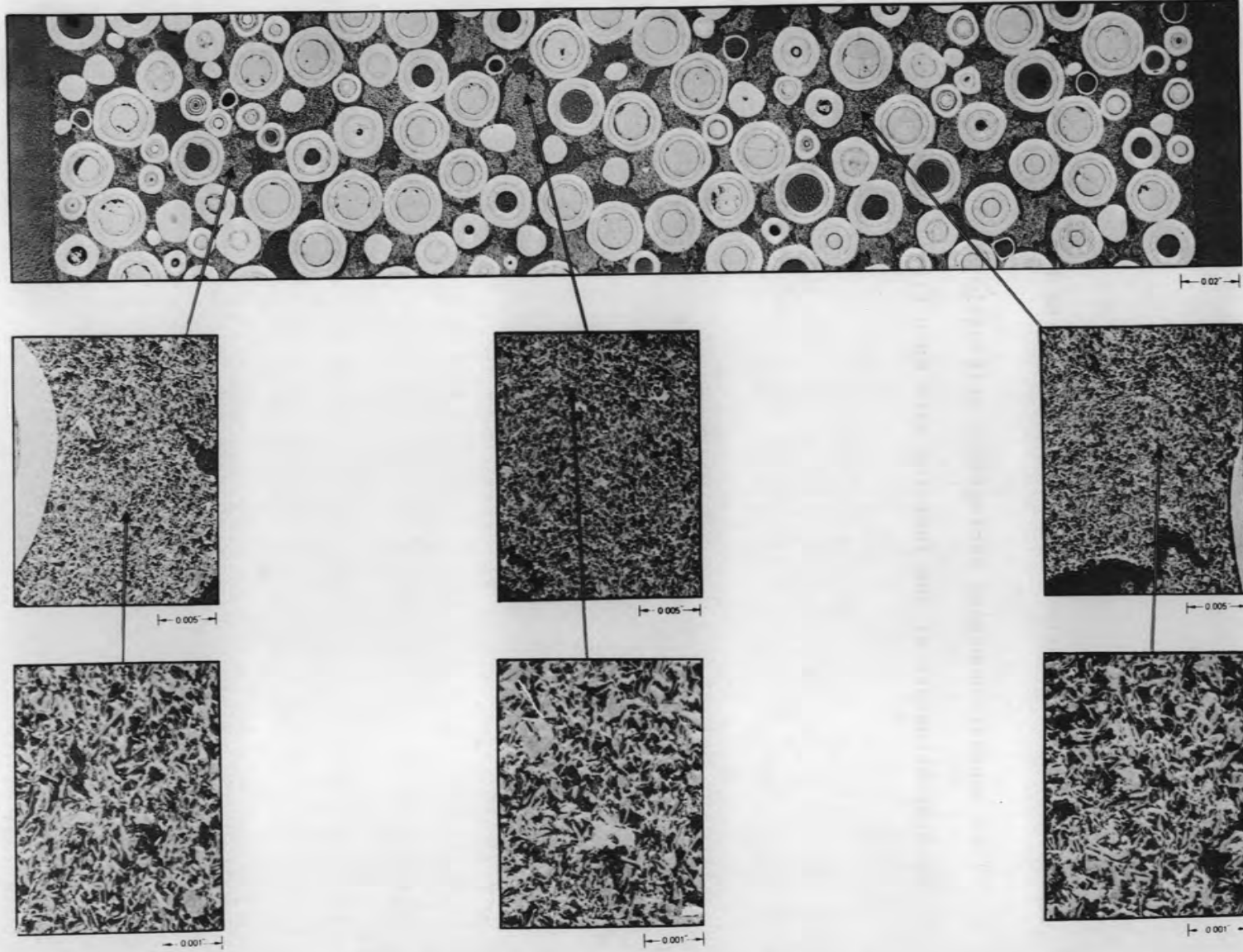


Fig. D-1. Microstructure of PTE fuel rod containing fissile particle type 1.

ITEM 2

PHOTO Y-112240

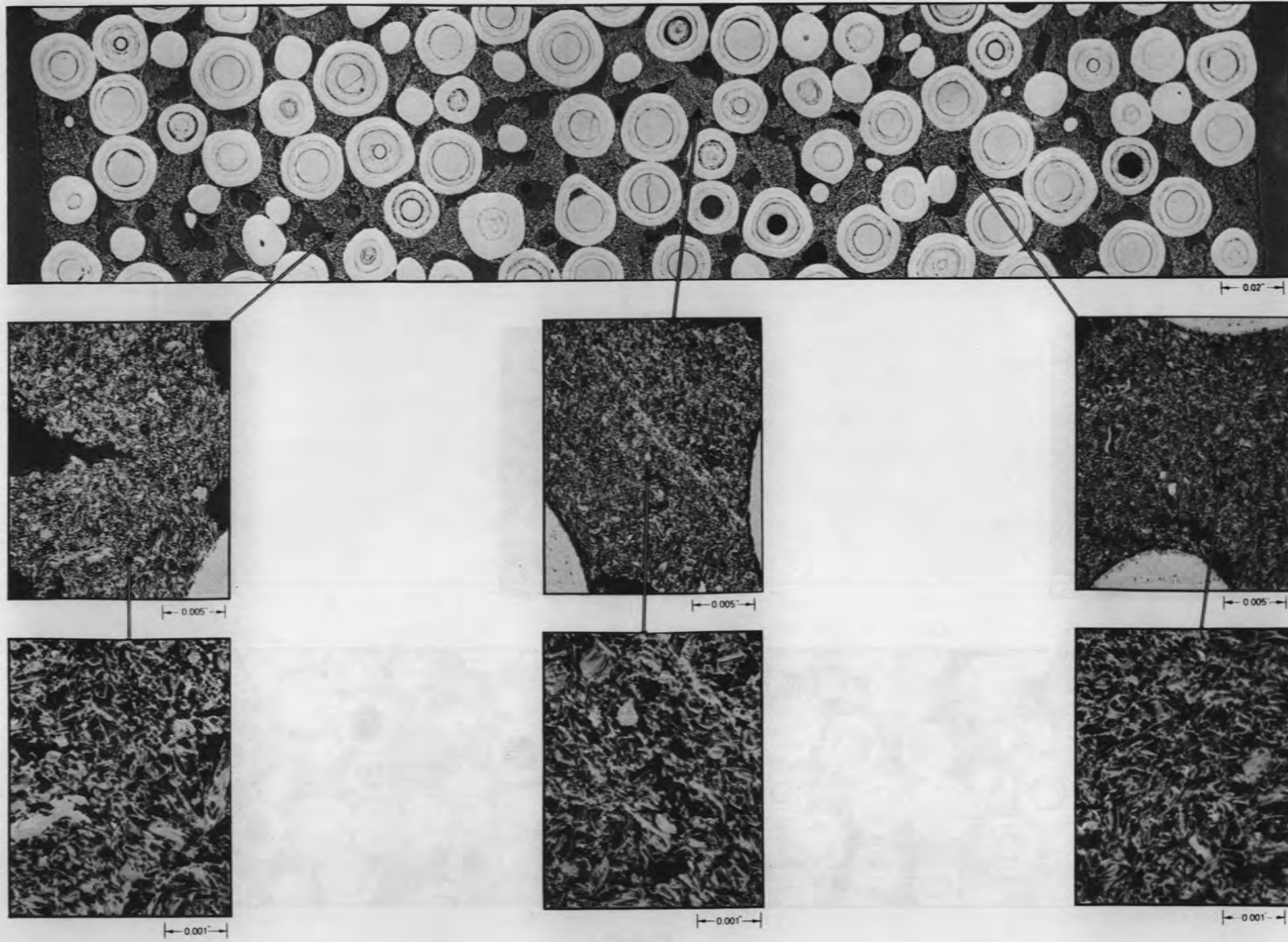


Fig. D-2. Microstructure of PTE fuel rod containing fissile particle type 2.

ITEM 4

PHOTO Y-112241

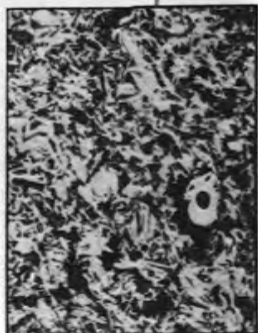
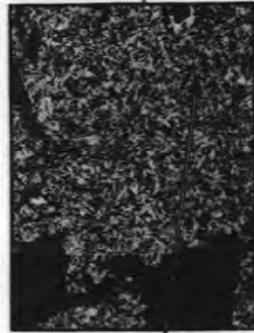
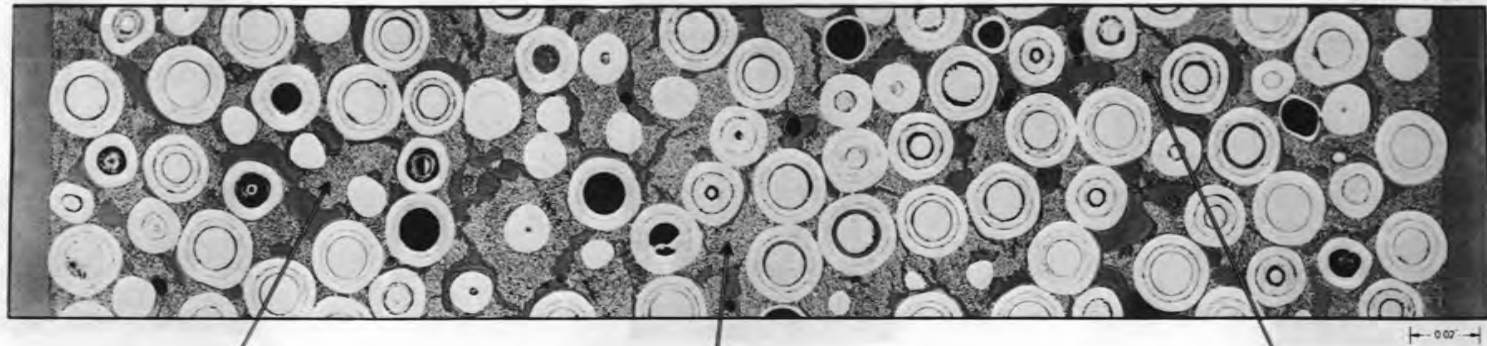
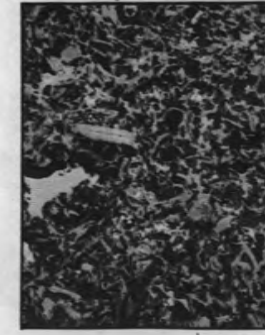
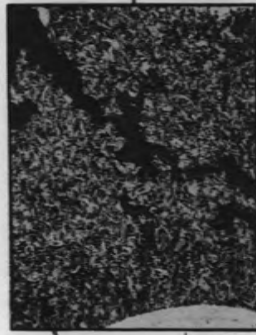
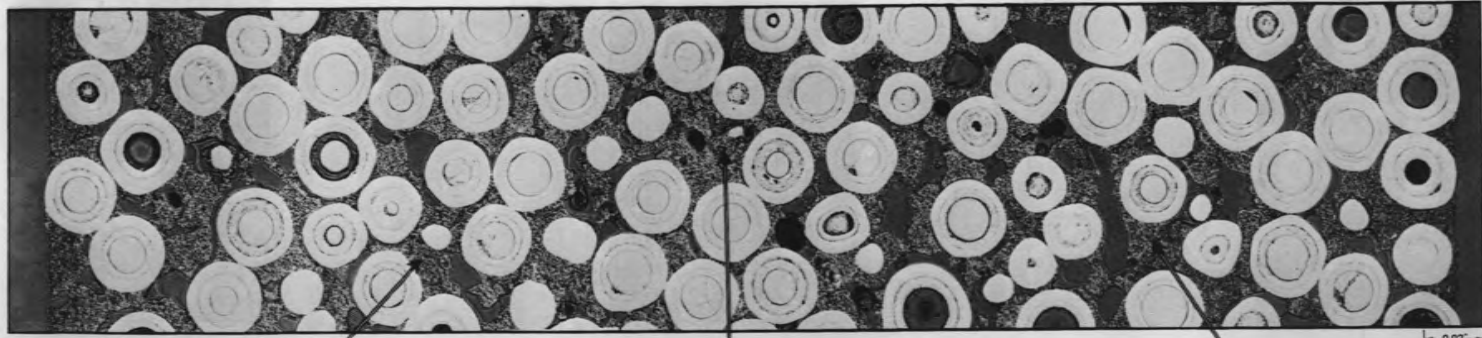


Fig. D-3. Microstructure of PTE fuel rod containing fissile particle type 4.

ITEM 5

PHOTO Y-112242



55

Fig. D-4. Microstructure of PTE fuel rod containing fissile particle type 5.

ITEM 6

PHOTO Y-112243

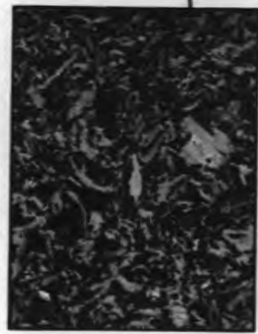
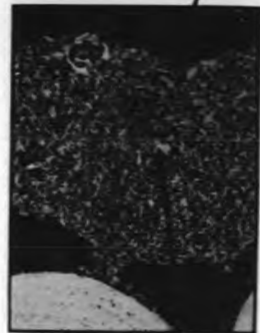
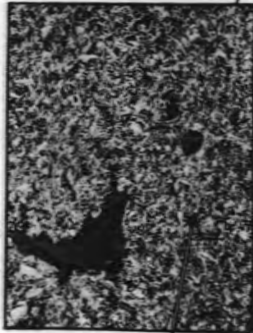
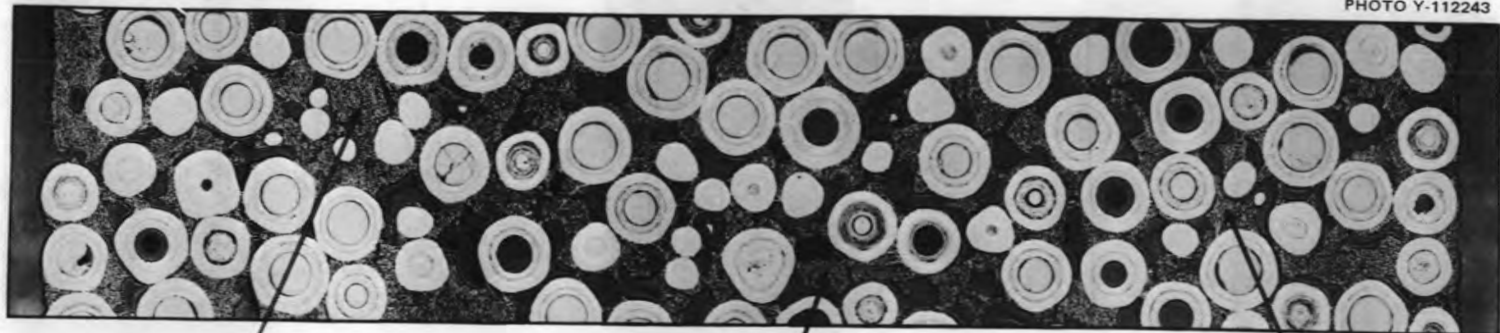


Fig. D-5. Microstructure of PTE fuel rod containing fissile particle type 6.

APPENDIX E

Photographs of Fuel Rods for PTE

This appendix contains photographs of each fuel rod loaded in the PTE. The top left rod is the bottom rod and the top right is next to the bottom, etc., until the bottom right rod is the top rod.

PHOTO Y-112317

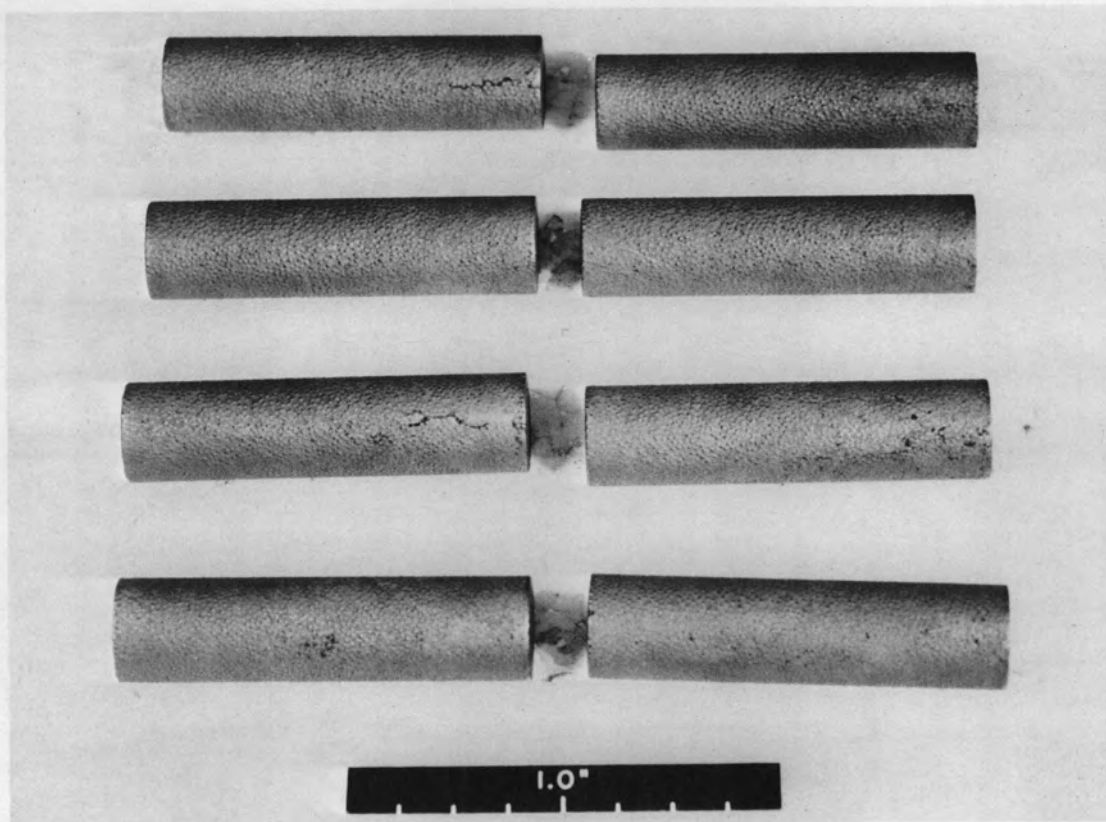
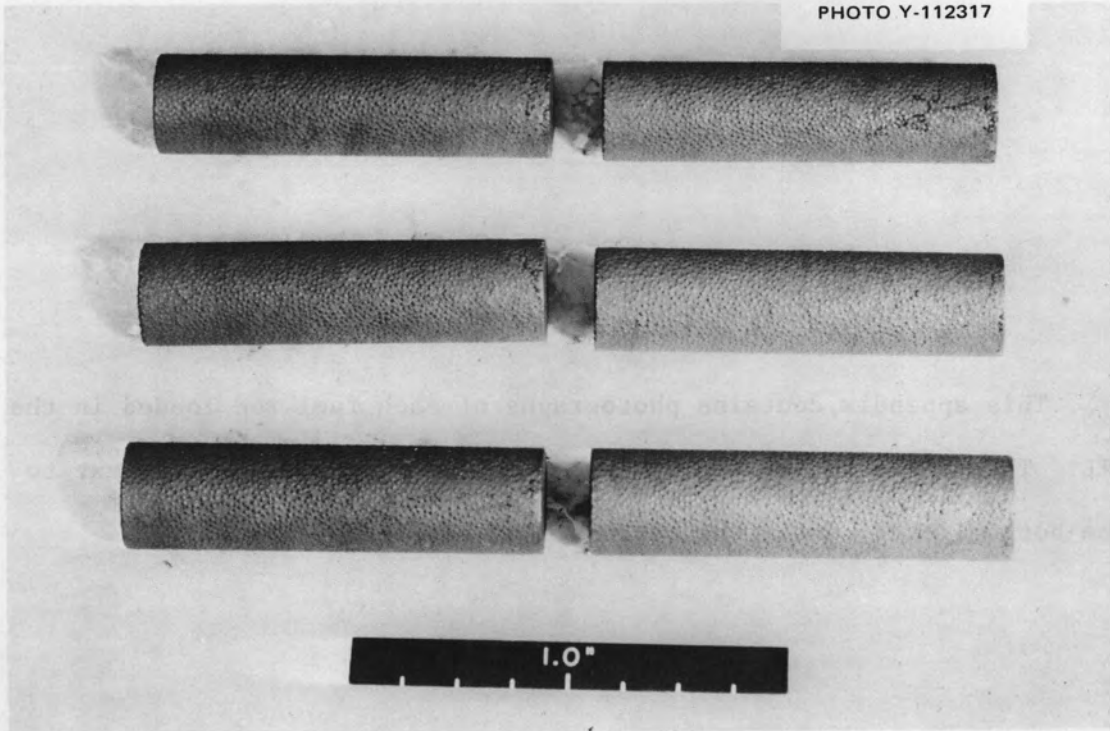


Fig. E-1. Fuel rods for PTE hole 1, particle type 5.

PHOTO Y-112318

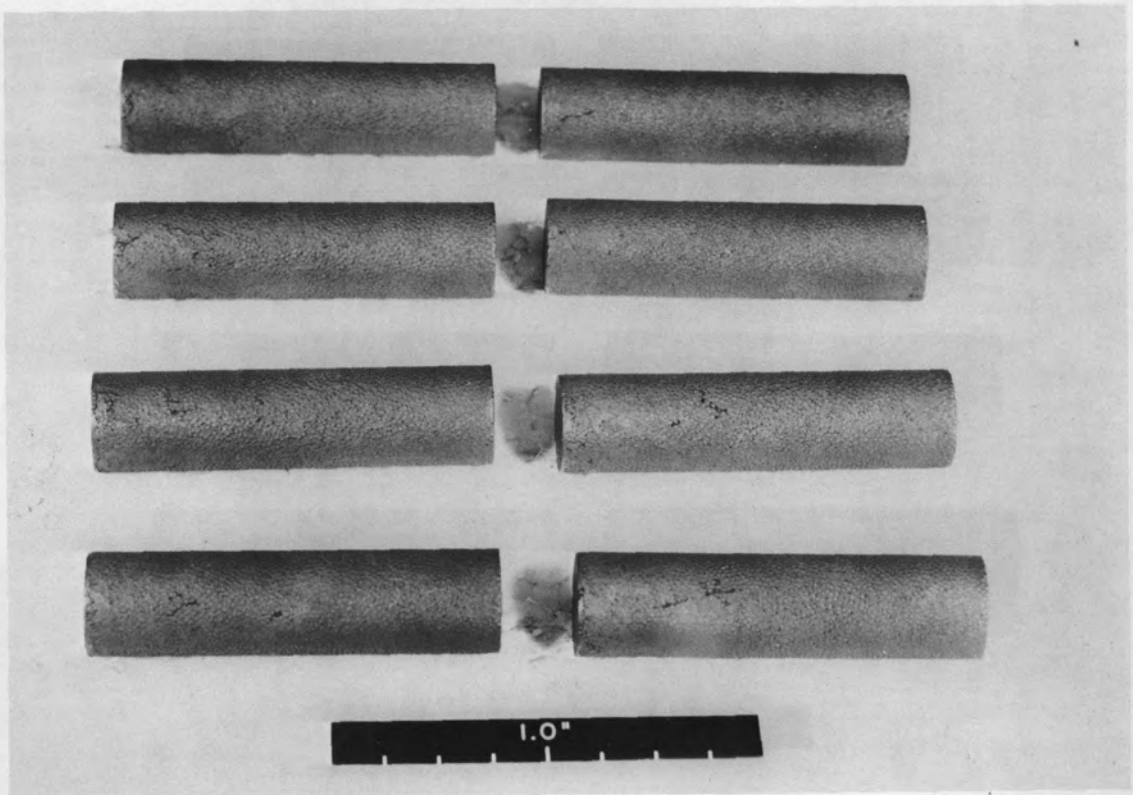
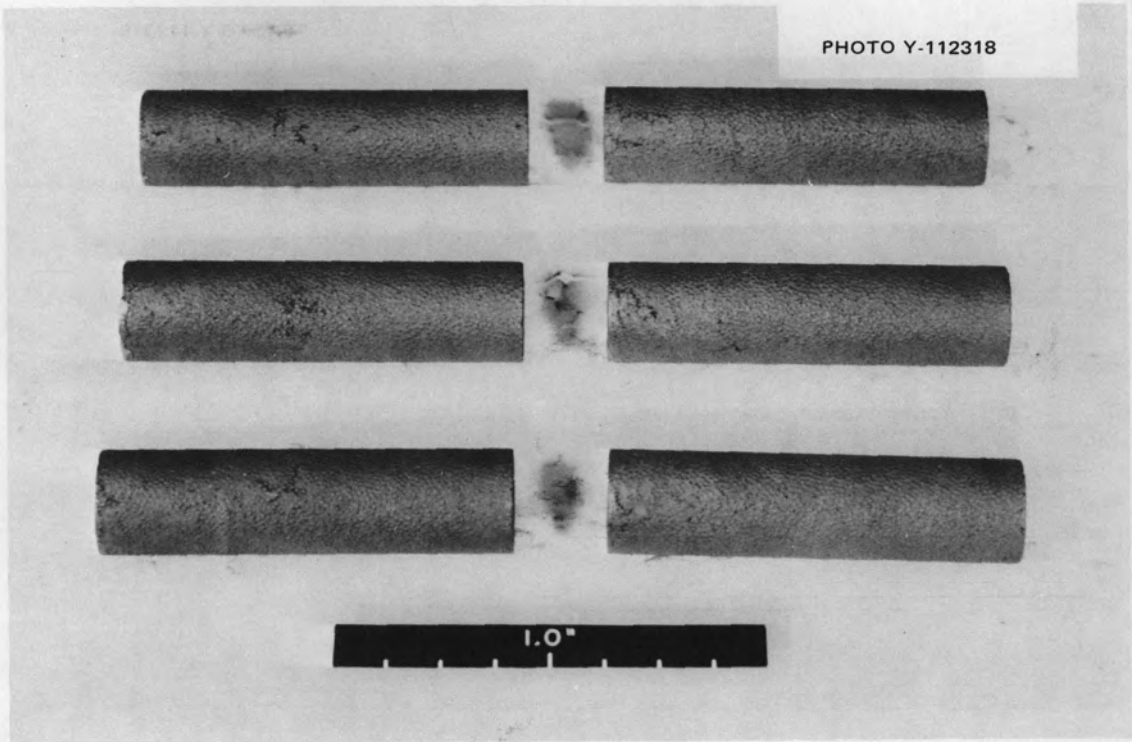


Fig. E-2. Fuel rods for PTE hole 2, particle type 6.

PHOTO Y-112319

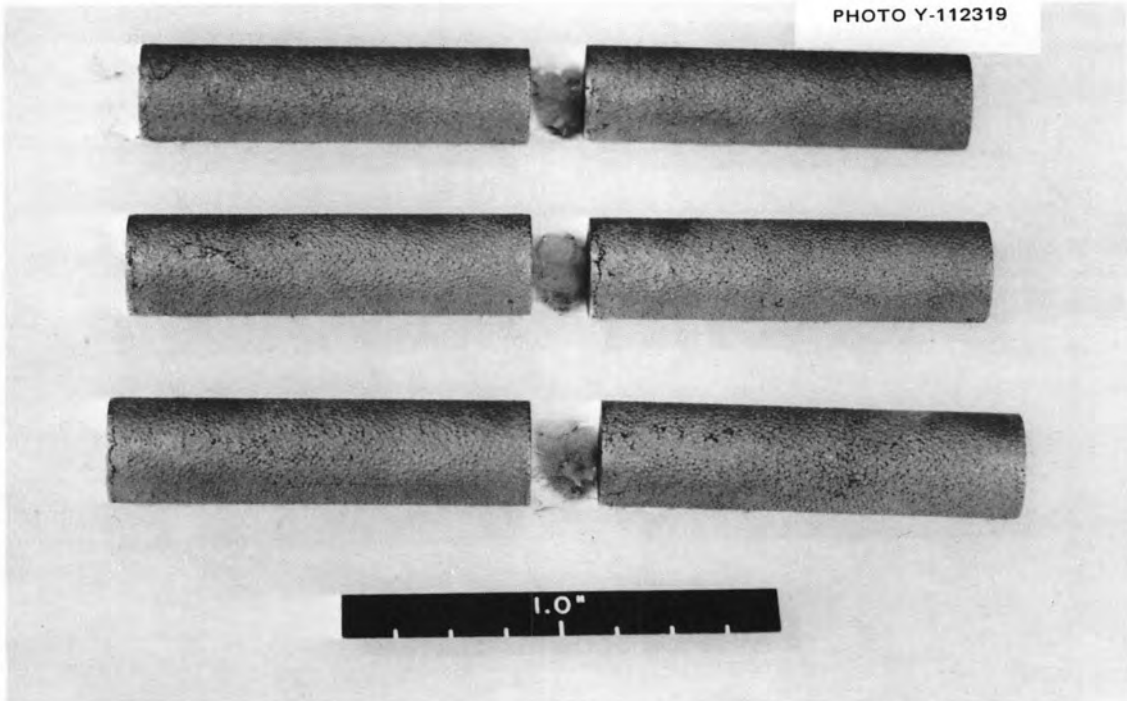


Fig. E-3. Fuel rods for PTE hole 3, particle type 6.

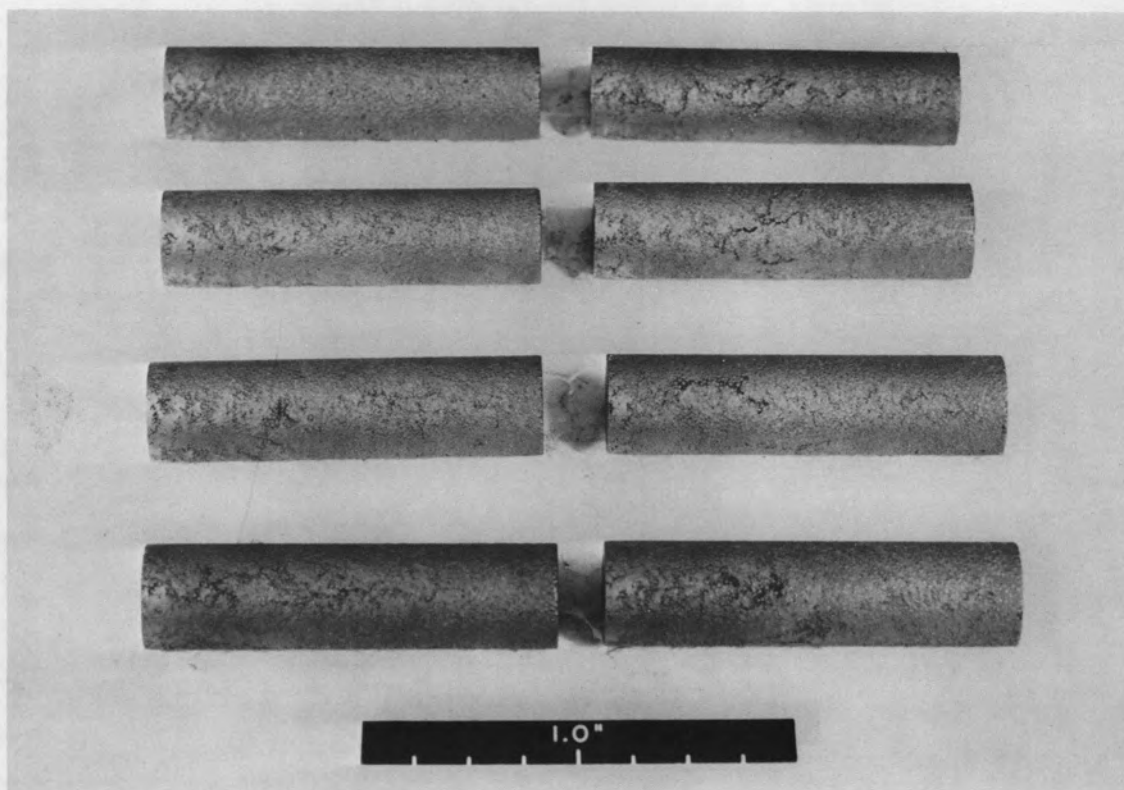


Fig. E-4. Fuel rods for PTE hole 4, particle type 1.



Fig. E-5. Fuel rods for PTE hole 5, particle type 1.

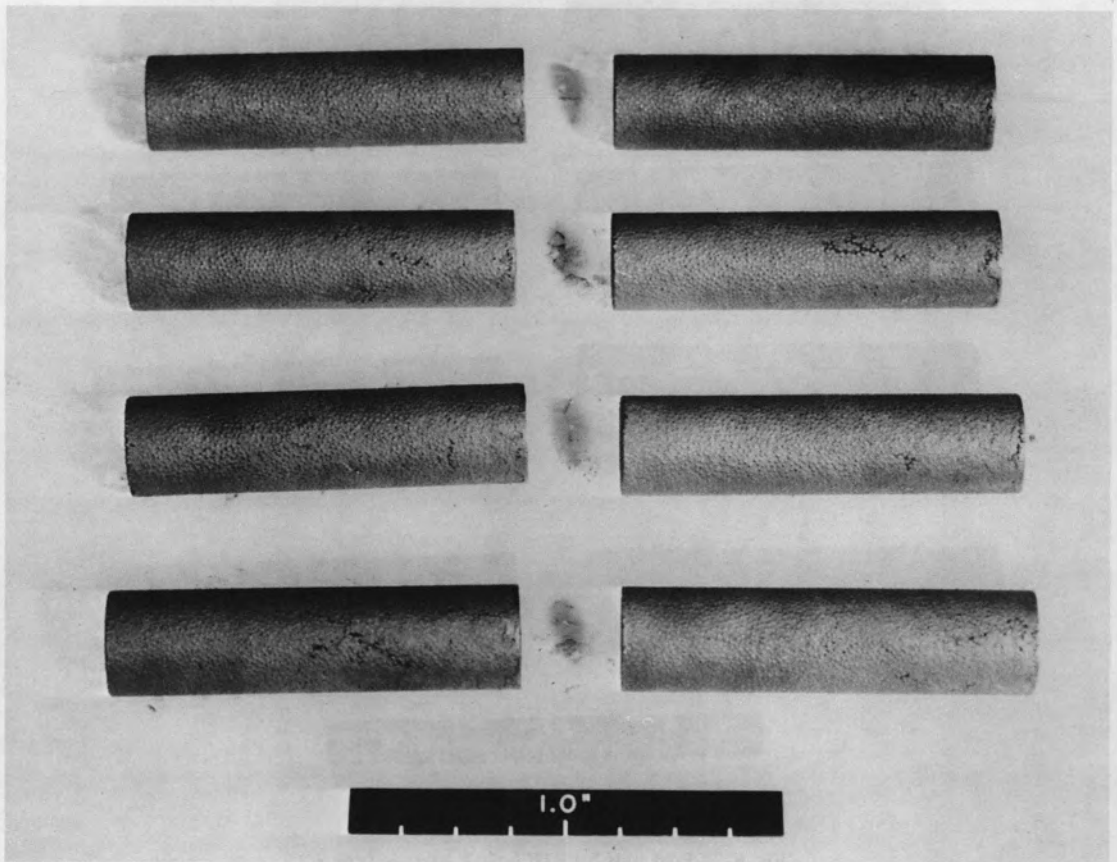
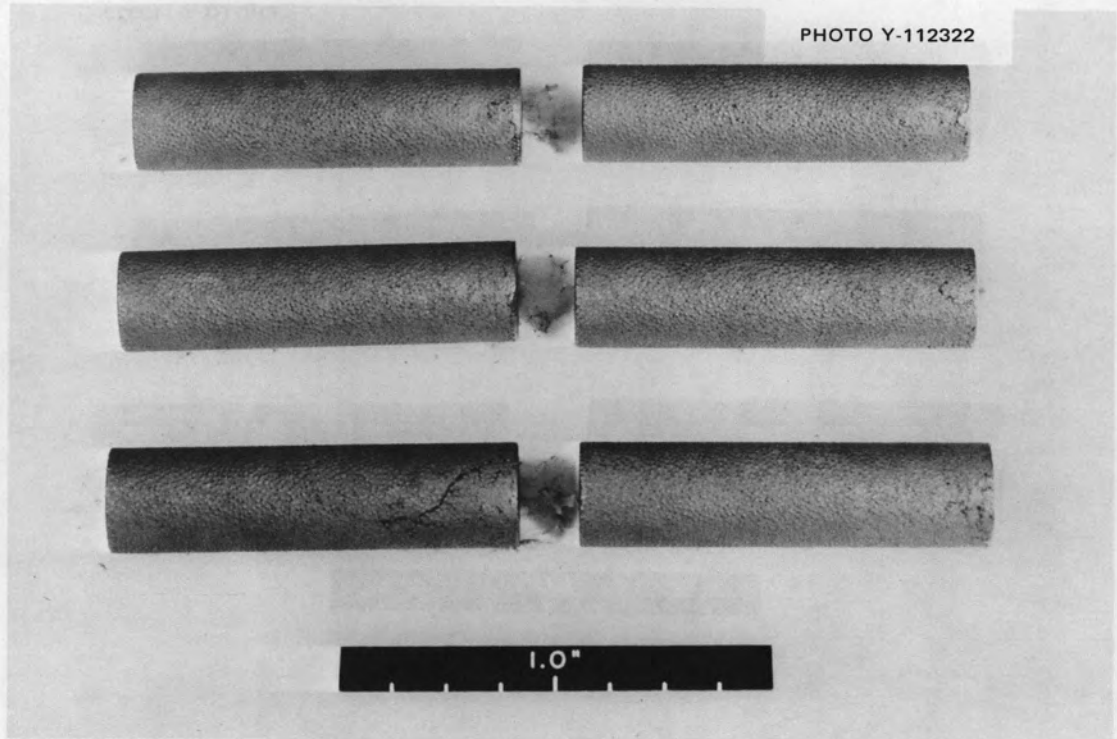


Fig. E-6. Fuel rods for PTE hole 6, particle type 4.

PHOTO Y-112323

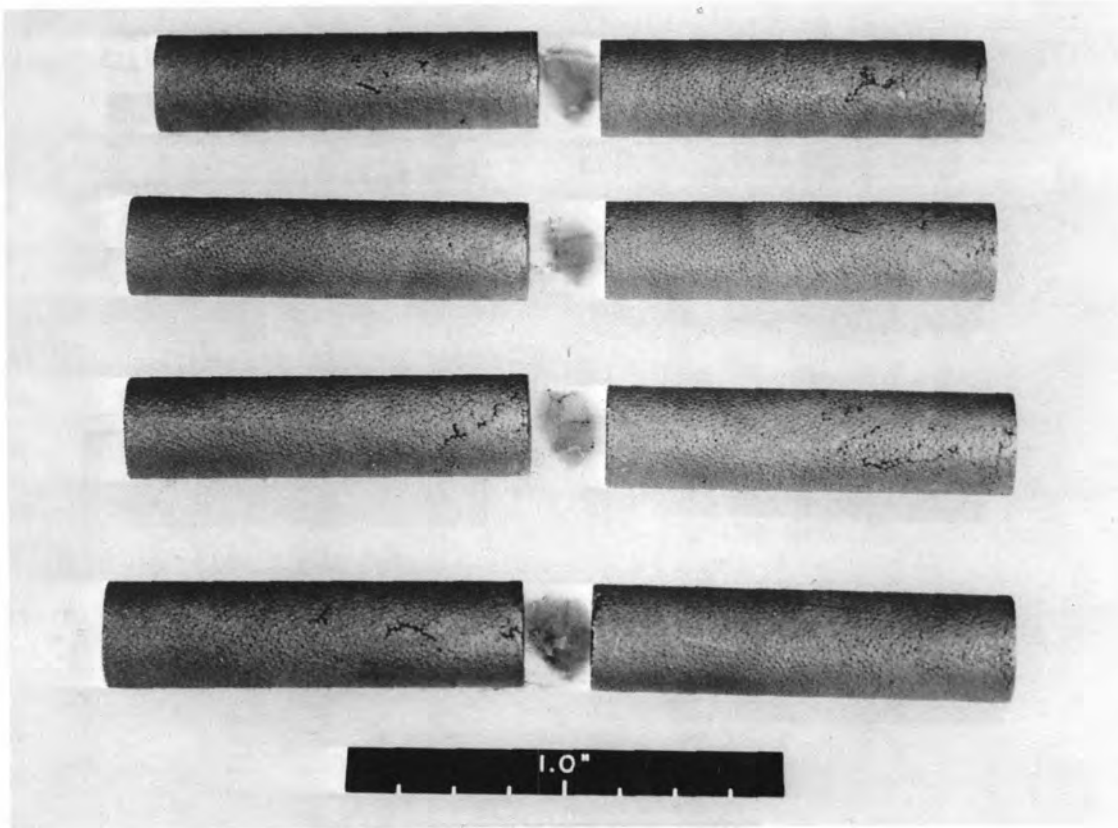


Fig. E-7. Fuel rods for PTE hole 7, particle type 2.

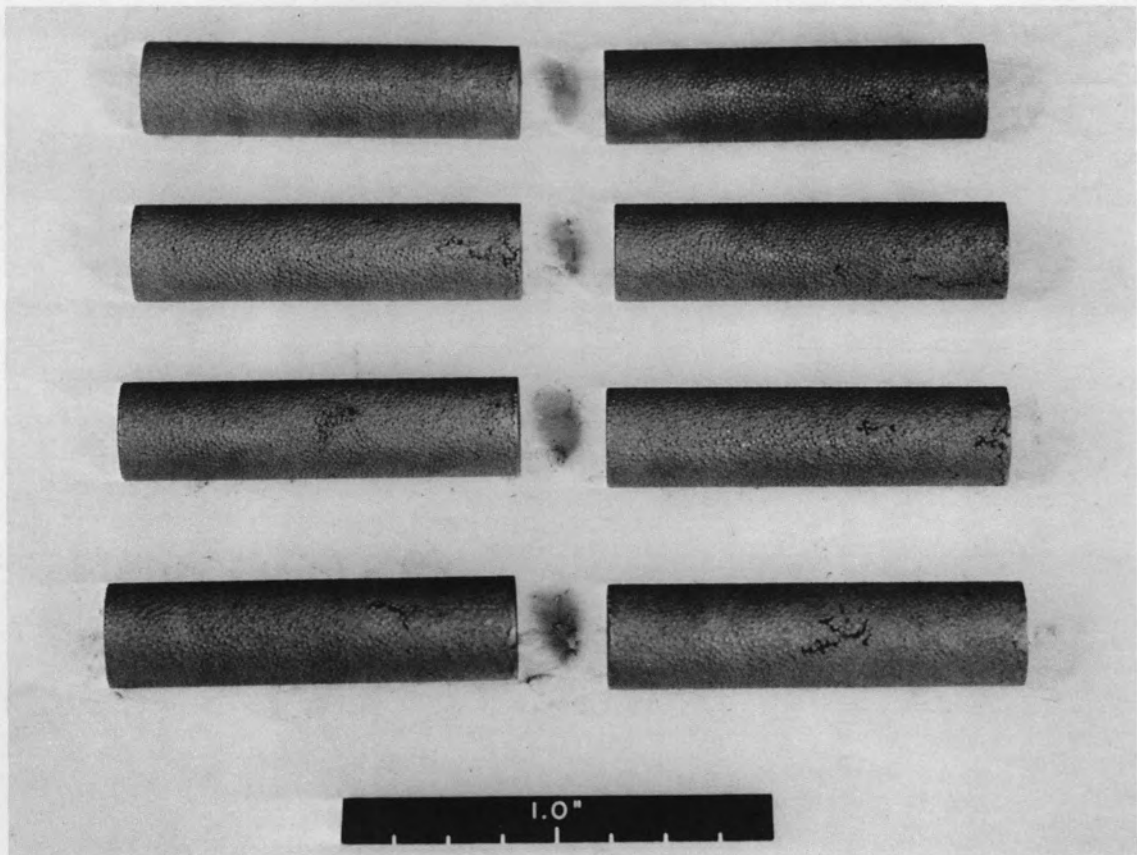
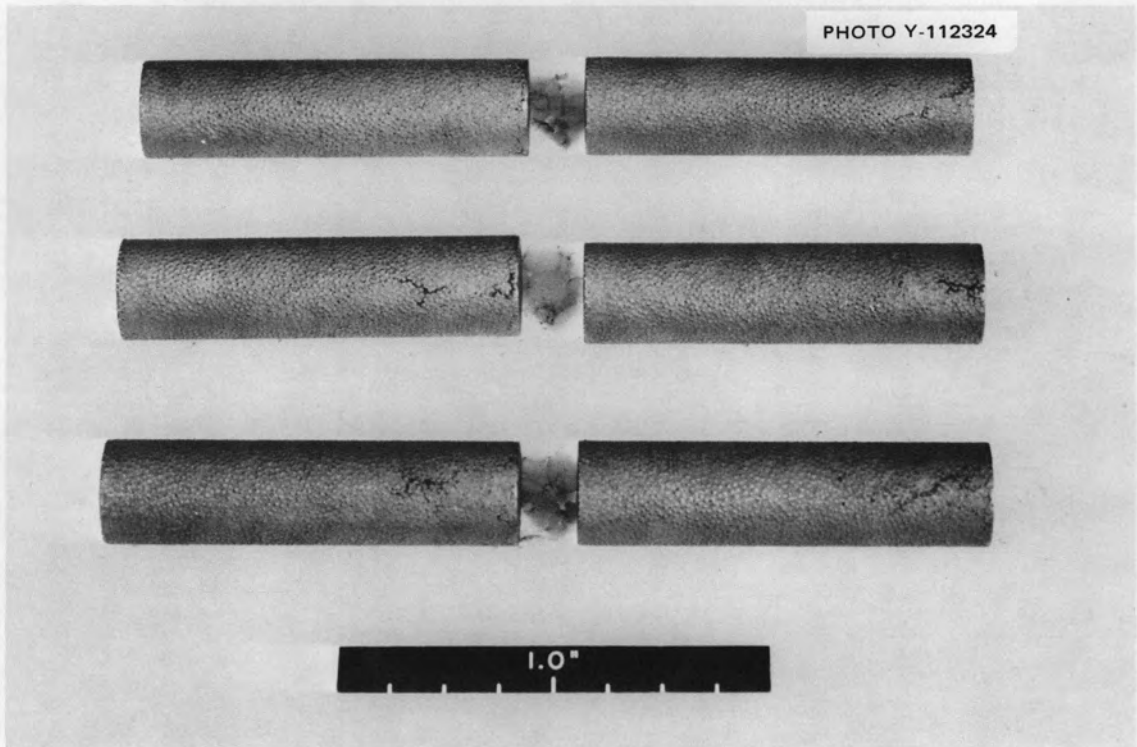


Fig. E-8. Fuel rods for PTE hole 8, particle type 5.



INTERNAL DISTRIBUTION
(79 copies)

Central Research Library (2)
ORNL - Y-12 Technical Library
Document Reference Section
Laboratory Records Department (5)
Laboratory Records, ORNL R.C.
G. M. Adamson, Jr.
J. W. Anderson
S. E. Beall
M. Bender
L. L. Bennett
R. E. Blanco
E. S. Bomar
R. A. Bradley
R. E. Brooksbank
~~W. E. Browning, Jr.~~
D. D. Cannon
H. P. Carter
H. E. Cochran
J. H. Coobs
F. L. Culler
C. W. Cunningham
J. E. Cunningham
F. C. Davis
H. J. de Nordwall
W. P. Eatherly
D. E. Ferguson
R. B. Fitts

~~J. H. Frye, Jr.~~
R. J. Gray
P. A. Haas
R. L. Hamner
R. F. Hibbs
M. R. Hill (3)
F. J. Homan (2)
S. I. Kaplan
P. R. Kasten (10)
W. J. Lackey
T. B. Lindemer
A. L. Lotts (5)
W. T. McDuffee
M. T. Morgan
R. B. Parker
W. H. Pechin
~~C. B. Pollock~~
J. M. Robbins
~~C. F. Sanders (2)~~
J. L. Scott
J. D. Sease (5)
J. W. Snider
D. B. Trauger
A. M. Weinberg
J. R. Weir
J. C. White
R. G. Wymer

EXTERNAL DISTRIBUTION
(49 copies)

AEC Technical Information Center, ORO
(17) Manager (for transmittal to members of ACRS)
(2)

AEC, ORO
Research and Technical Support Division
Patent Office

AEC Site Representative, ORNL
D. F. Cope
~~F. E. Deering~~

AEC, Washington, D.C. 20545
(3) F. O'Leary, Director of Licensing
R. E. Pahler
(2) R. Rogers, Director of Regulatory Standards
O. T. Roth

Gulf General Atomic Company, P.O. Box 81608, San Diego, California 92112
R. C. Dahlberg
J. B. Radcliffe
(10) H. B. Stewart
W. V. Goeddel
(5) T. D. Gulden
D. A. Nehrig